Missouri S&T Library and Learning Resources

Scholars' Mine

Masters Theses

Student Theses and Dissertations

Summer 2016

PIM source identification using vibration modulation method

Sen Yang

Follow this and additional works at: https://scholarsmine.mst.edu/masters_theses

Part of the Electrical and Computer Engineering Commons

Department:

Recommended Citation

Yang, Sen, "PIM source identification using vibration modulation method" (2016). *Masters Theses*. 7731.
https://scholarsmine.mst.edu/masters_theses/7731

This thesis is brought to you by Scholars' Mine, a service of the Missouri S&T Library and Learning Resources. This work is protected by U. S. Copyright Law. Unauthorized use including reproduction for redistribution requires the permission of the copyright holder. For more information, please contact scholarsmine@mst.edu.

PIM SOURCE IDENTIFICATION USING VIBRATION MODULATION METHOD

by

SEN YANG

A THESIS

Presented to the Faculty of the Graduate School of

MISSOURI UNIVERSITY OF SCIENCE AND TECHNOLOGY

In Partial Fulfillment of the Requirements for the Degree

MASTER OF SCIENCE IN ELECTRICAL ENGINEERING

2016

Approved by

David Pommerenke, Advisor
Victor Khilkevich
Jun Fan

© 2016
SEN YANG
All Rights Reserved

ABSTRACT

In Section 1, passive intermodulation (PIM) is introduced and the mechanism of it is briefly explained. Then, the up-to-date PIM testing and source identification method in the industrial and academia worlds will be summarized.

The vibration modulation method for PIM source identification is proposed in Section 2. Different vibration sources were tested and compared, and the test results showed that the vibration modulation method is able to identify PIM source with good accuracy.

Section 3 outlines a special PIM source identification system built based on the vibration modulation system. The two subsystems, PIM receiver and PIM vibrator, are illustrated in detail.

In Section 4, PIM source identification tests were conducted on a base station antenna using the PIM source identification system. The experiment results show the system was able to pinpoint the PIM source accurately.

ACKNOWLEDGMENTS

I would like to express my deepest gratitude to my advisor, Prof. David Pommerenke, for his excellent guidance and patience. His passions on EMC and ESD areas inspired me to set my research path on this challenging field. Without his strong support, I would never have been able to finish my dissertation.

I would like to thank Dr. Jun Fan and Dr. Victor Khilkevich for their valuable support and advice during my study in EMCLAB.

I would also like to thank all other faculty members and student colleagues in EMCLAB. Their enthusiasm over EMC and SI problems and their kind support inspire me to move forward over all those obstacles step by step.

Finally, I am deeply grateful for the ultimate support and understanding from my family. I would give especial thanks to my wife, Qian Liu, for all the years we have come through and for all the years to experience in the future.

TABLE OF CONTENTS

Page

ABSTRACT iii

ACKNOWLEDGMENTS iv

LIST OF ILLUSTRATIONS vii

LIST OF TABLES x

SECTION

1. INTRODUCTION 1

1.1. BRIEF INTRODUCTION TO PIM 1

1.2. CHARACTERIZATION OF PIM 1

1.3. WAYS TO PINPOINT THE SOURCES OF PIM 3

1.4. BASE STATION ANTENNA PIM PROBLEMS: PRESENT, DEVELOPING TRENDS AND RELATED CHALLENGES 4

1.5. OTHER METHODS IN ACADEMIA (NEAR-FIELD SCANNING) 4

1.6. NEAR-FIELD SCANNING EXPERIMENT 6

2. VIBRATION MODULATION METHOD 9

2.1. METHOD DESCRIPTION 9

2.2. MEASUREMENT WITH LOOSE CONNECTORS 13

2.2.1. DC Motor.. 14

2.2.2. Buzzer. 14

2.2.3. Audio Speaker. 14

2.2.4. Ultrasonic Transducer. 14

2.3. MEASUREMENT RESULTS AND ANALYSIS WITH LOOSE CONNECTORS 18

2.4. MEASUREMENT ON BASE STATION ANTENNA 20

2.5. ANTENNA PIM LEVEL MEASUREMENT 20

2.5.1. Ferrite Debris As PIM Source. 21

2.5.2. Investigation of PIM Problem Caused By Vibration. 24

2.6. VIBRATION METHOD ON BASE STATION ANTENNA ARRAY 24

2.7. MEASUREMENT RESULTS AND ANALYSIS OF BASE STATION ANTENNA 27

3. PIM SOURCE IDENTIFICATION SYSTEM 31
3.1. PIM RECEIVER 31
3.1.1. PGA103+ LNA Module. 32
3.1.2. SAW Filter Bank.. 35
3.1.3. Mixer. 35
3.1.4. MAX2870 Frequency Synthesizer. 35
3.1.5. 433.92 MHz SAW Filter. 36
3.1.6. Variable Bandwidth Filter Bank. 36
3.1.7. Second Stage Adjustable Amplifier. 39
3.1.8. Amplifier ZKL-1R5+. 41
3.1.9. Splitters. 42
3.1.10. Detectors. 42
3.1.11. Touchscreen Control Panel. 43
3.1.12. System Integration.. 44
3.2. PIM ANALYZER 45
3.2.1. Self-made PIM Analyzer. 45
3.2.2. Modified PIMPro 1921. 46
3.3. PIM VIBRATION SYSTEM 49
3.3.1. Ultrasonic Driver. 51
3.3.2. Vellaman 200 W Power Amplifier. 51
3.3.3. Ultrasonic Transducer. 51
4. PIM VIBRATION SYSTEM TEST AND METHOD VALIDATION 53
4.1. PIM SOURCE IDENTIFICATION - FERRITE DEBRIS 54
4.2. PIM SOURCE IDENTIFICATION - LOOSE SCREWS 56
4.3. CONCLUSION 57
4.4. FUTURE WORK 58
BIBLIOGRAPHY 59
VITA. 62

LIST OF ILLUSTRATIONS

Page

Figure 1.1. Typical PIM testing setup. 2
Figure 1.2. Normalization of the PIM near-field measurement 5
Figure 1.3. Block diagram of the PIM near-field measurement equipment 6
Figure 1.4. Measurement set-up for near-field scanning. 7
Figure 2.1. Amplitude modulation of modulated PIM signal when vibrating at PIM source. 9
Figure 2.2. System diagram of vibration method. 10
Figure 2.3. Kaelus PIM analyzer. 11
Figure 2.4. Rohde & Schwarz Spectrum Analyzer equipped with video output. 11
Figure 2.5. Audio amplifier for amplifying RF output of PIM tester. 12
Figure 2.6. Vibrating at PIM source. 12
Figure 2.7. Measurement set-up of the vibration method. 13
Figure 2.8. Kaelus Low PIM 50 Ohm load and its parameters. 13
Figure 2.9. Two vibration locations on the DUT (two piece of coax cable). 14
Figure 2.10. DC motor and its parameters. 15
Figure 2.11. Illustration on how the DC motor was mounted to the cable. 15
Figure 2.12. The buzzer and its parameters 15
Figure 2.13. Illustration on how the buzzer was mounted to the cable. 16
Figure 2.14. Two types of speakers that were used in the measurement. 16
Figure 2.15. Signal generator to drive the speaker to operation frequency. 16
Figure 2.16. Ultrasonic transducer and its parameters. 17
Figure 2.17. Apex MP118 evaluation kit to drive the transducer. 17
Figure 2.18. A holder was used to support the transducer. 18
Figure 2.19. Electrical properties of the base station antenna. 21
Figure 2.20. Antenna dimensions and mechanical properties. 21
Figure 2.21. Reflection (S11, S22) 21
Figure 2.22. Isolation (S12, S21). 22
Figure 2.23. Antenna PIM level measurement set-up 22
Figure 2.24. Antenna set-up. 22

Figure 2.25. Small ferrite piece attached to the center of dipole antenna. 23
Figure 2.26. DC motor was placed to different places on the base station antenna. 24
Figure 2.27. PIM source I: ferrite debris. 24
Figure 2.28. PIM source II: metal debris. 25
Figure 2.29. PIM source III: bad soldering. 25
Figure 2.30. Potential PIM source location I: Solder joint. 25
Figure 2.31. Potential PIM source location II: E-downtilt (phase shifter). 26
Figure 2.32. Vibration tool I: speaker. 26
Figure 2.33. Vibration tool II: ultrasonic transducer. 26
Figure 3.1. PIM Receiver system schematic. 32
Figure 3.2. PGA103+ gain vs. frequency. 33
Figure 3.3. Gain compensation circuit. 33
Figure 3.4. Schematic of first stage amplifier. 34
Figure 3.5. S21 measurement results for the first stage amplifier with external 40dB attenuation. 34
Figure 3.6. Cellular SAW filter bank circuit diagram. 35
Figure 3.7. SA measurement results for 1880 MHz and 1747 MHz SAW filters. 37
Figure 3.8. Schematic of mixer. 37
Figure 3.9. Assembled frequency synthesizer board. 38
Figure 3.10. Schematic of 433.92 MHz SAW filter and measurement results. 38
Figure 3.11. Measured S21 of the 433.92 MHz SAW filter 39
Figure 3.12. Bandpass filter with parameters optimized in ADS. 39
Figure 3.13. Circuit diagram of variable BW filter bank. 40
Figure 3.14. S21 of different filters. 40
Figure 3.15. Schematic of second stage adjustable amplifiers. 41
Figure 3.16. Manufacture board of second stage adjustable amplifiers with box. 41
Figure 3.17. Mini-Circuits ZKL-1R5+ 10 to 1500 MHz 40 dB gain amplifier 41
Figure 3.18. ZFSCJ-2-4+ 2-way splitter. 42
Figure 3.19. ZA3CS-400-3W+ 3-way splitter. 42
Figure 3.20. Schematic of log detector and measurement result. 42

Figure 3.21. Schematic of linear detector and measurement result. 43
Figure 3.22. SmartGLCD touchscreen panel. 43
Figure 3.23. First screen of user interface. 44
Figure 3.24. Second screen of user interface 44
Figure 3.25. Integrated PIM receiver in an aluminum chassis. 45
Figure 3.26. Block diagram of self-made PIM analyzer. 45
Figure 3.27. Two power amplifier purchased for the self-made PIM analyzer. 46
Figure 3.28. CCI PIMPro 1921 PIM analyzer. 47
Figure 3.29. Internal structure of the purchased PIM analyzer. 47
Figure 3.30. Rx module of the PIM analyzer. 48
Figure 3.31. Modified analyzer with coax probe added for Rx (PIM) signal output. 48
Figure 3.32. Illustration of the effect of different phase noise level. 49
Figure 3.33. Block diagram of the modified PIM analyzer. 49
Figure 3.34. Completed modification of PIM analyzer. 50
Figure 3.35. Photo of completed PIM analyzer modification. 50
Figure 3.36. MP118 power opamp with power supplies integrated in an aluminum chassis. 51
Figure 3.37. Assembled vibrator driver with VM100 power amplifier module. 52
Figure 3.38. PIM vibrator system. 52
Figure 4.1. Block diagram of measurement set-up. 53
Figure 4.2. Set-up photo of vibration modulation method with base station antenna. 54
Figure 4.3. Ferrite debris as PIM source on power divider. 55
Figure 4.4. Vibration on different locations 55
Figure 4.5. Inner structure of E-downtilt (phase shifter). 56
Figure 4.6. Loose screw on the phase shifter as PIM source 56
Figure 4.7. Vibrating at different locations on phase shifter. 57
Figure 4.8. Ultrasonic transducer with ceramic rod structure 58

LIST OF TABLES

Page

Table 1.1. List of representative manufacturer and equipment of locating PIM source 3

Table 1.2. Near-field scanning when the PIM source existed on #7 in front of the base station antenna 8

Table 2.1. Comparison of different vibration sources 19

Table 2.2. PIM level of different ferrite placement 23

Table 2.3. Case III – Bad solder joint 27

Table 2.4. PIM source - Ferrite piece 28

Table 2.5. PIM source - Metal debris at the solder joint 29

Table 2.6. PIM source - Metal debris in E-downtilt 30

Table 3.1. SAW filters for different cellular bands 36

Table 3.2. Measurement results at 900 MHz RF frequency 38

Table 3.3. Measurement results at 1900 MHz RF frequency 38

Table 3.4. ECS crystal filter parameters 39

1. INTRODUCTION

1.1. BRIEF INTRODUCTION TO PIM

Passive intermodulation (PIM) is a form of intermodulation distortion. The intermodulation occurs in nonlinear systems, which are generally composed of active components. Passive devices such as cables, connectors, and antennas are usually considered to be linear devices. PIM, however, occurs in passive devices which are subject to two or more high power tones. Because of the extreme weak nonlinearity in passive devices, the typical PIM level is as small as -120 to -160 dBc.

PIM is a growing concern for cellular network operators. This is because PIM can create interference that will reduce the receiving sensitivity of a cell site or even block call connections. This interference can affect both the unit that creates it, as well as other nearby receivers. PIM is created by a high power transmitter, thus, on-site PIM testing has to be done at or above the original transmitter power levels to ensure that the test reveals potential PIM issues. High-speed digital data communications make PIM testing critical. As cell usage and throughput grows, the peak power produced by the new digital modulations increases dramatically, contributing heavily to PIM problems.

PIM can be induced by multiple sources. The following sources have been reported: 1) Usage of magnetic material, such as nickel.Bad contacts in the current path. 2) Contamination with metallic particles: metallic particles that are located, for example, in a coax cable after soldering, are subjected to the strong field, but have weak electrical contact causing PIM

Investigation on PIM sources can be found in numerous articles, including [1][2][3][4][5][7].

1.2. CHARACTERIZATION OF PIM

The nonlinearity can produce forward and backward PIM products. Forward PIM means the portion of PIM products produced are transmitted from the DUT. Backward PIM means the portion of PIM products produced are reflected back to the DUT. In practice, only reflected PIM products are often measured since they interfere with the Rx signals [26].

Mechanical, environmental, and electrical factors can influence the performance of the device. In the field, any mechanical flexing due to wind and vibration can have a devastating impact. In order to test for this before the assembly is installed, dynamic PIM tests are being developed by the IEC [8]. Raw cable and final cable assemblies will be subjected to flexing and rotational movement using a fixture such as the one shown in Figure 1.1 (a). Connectors will be arranged in very short cable assemblies and subjected to an impact test from a free falling weight as shown in Figure 1.1 (b). Temperature cycling and thermal shock can also have a significant effect on PIM and will likely be included in individual customer specifications [4].

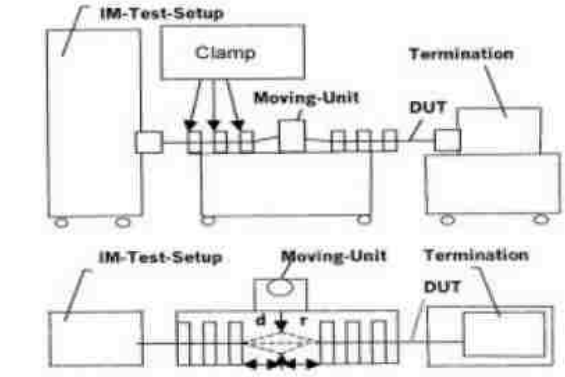

(a)

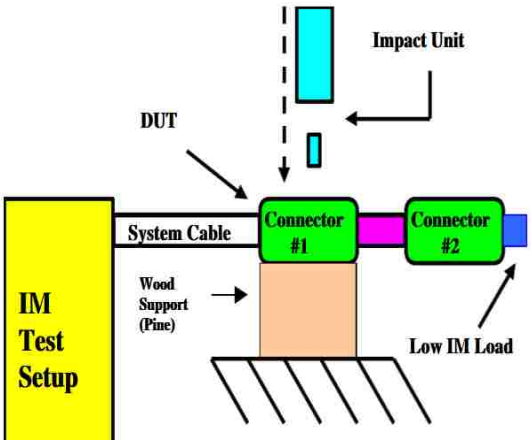

(b)

Figure 1.1. Typical PIM testing setup.
(a) Cable flexing fixture, (b) Connector test set-up.

1.3. WAYS TO PINPOINT THE SOURCES OF PIM

PIM sources can be located by many different methods. A traditional method is to manually tap/manipulate all possible locations. If the PIM level is affected by any of this manipulation then the location is determined to be a PIM source. Another approach is to replace components until the problem goes away, which is time-consuming and very costly; this approach appears to be the standard way of fixing PIM problems when technicians are unaware of the PIM test [1].

Several PIM analyzer suppliers have developed a range-to-fault (RTF) technology that includes the additional hardware and signal processing software to generate time-domain plots similar to those generated in network analysis distance-to-fault. RTF technology is an analysis tool developed to enhance, not replace, standard fixed tone PIM testing [11][15]. RTF works by transmitting two 20 W (+43 dBm) test frequencies into the system under test. One test frequency is fixed while the second frequency is swept over a certain range of frequencies to produce IM products in the receive band of the system under test. Since RTF analysis requires high power signals to be swept outside the operator's licensed spectrum, this test should only be conducted on systems that are terminated into a low PIM load to prevent interference. The inverse FFT algorithm is used to reconstruct time-domain range pulses by digitally summing the quantized phase and amplitude components of each frequency involved in the computation. The more bandwidth available for analysis, the sharper the mathematical pulse edges will be. Table 1.1 shows the two suppliers that provide PIM source identification methods.

Table 1.1. List of representative manufacturer and equipment of locating PIM source

Company	Product	Locating PIM sources	Reference
Kaelus	iQA series	Range-to-Fault (RTF)	[11]
Anritsu	PIM Master	Distance-to-PIM (DTP)	[12]

1.4. BASE STATION ANTENNA PIM PROBLEMS: PRESENT, DEVELOPING TRENDS AND RELATED CHALLENGES

The antenna is one of the most important parts in all RF systems. If the antenna creates PIM, it will propagate along with the rest of the signal. If the antenna is also used for receiving, the created PIM signal will couple to the Rx channel and, thus, cause sensitivity to deteriorate. The growing complexity of modern antennas makes it more likely to cause PIM problems. Thus, it has become a common practice to test PIM performance before deploying the antenna on site [15].

1.5. OTHER METHODS IN ACADEMIA (NEAR-FIELD SCANNING)

There are other PIM testing methods in academia, such as near-field scanning [28]. The principle of the PIM near-field measurement is the same as in a common near-field measurement: the near-field measurement of PIM is performed to find the signal amplitude and phase at the PIM frequency of interest. It can then be used to localize the PIM sources in open devices and structures such as micro strip lines and antennas. The method is based on the idea that at the PIM frequency the reactive near-field will have a discontinuity in the vicinity of the distortion source. However, as stated before, this method could not locate the PIM sources in closed components like cables and cavity filters.

In the PIM scanner, two high power Tx signals are fed to the antenna under test (AUT) which is scanned with either an electric or magnetic field probe. This method has been demonstrated for the GSM900 frequency band and the equipment sensitivity has been improved down to -110 dBm with Tx signal of 2 x 43 dBm. The probe is moved close to the DUT, less than one tenth of a wavelength. However, instead of measuring the signal at the input frequency, the signal is measured at the PIM frequency of interest. The discontinuity will be shown in the measured data if the scanning area contains the PIM source (Figure 1.2). In Figure 1.2 (a), a small signal at 910 MHz is used as a calibration signal, $P_{cal,AUT}$; and in Figure 1.2 (b), two high-power Tx signals are fed to the AUT in the PIM signal measurement, P_{Tx1} and P_{Tx2}. A PIM source is located in the cable.

The block diagram of the measurement equipment is shown in Figure 1.3. The AUT, the receiver unit front end, and the linear guides are located inside a small shielded

anechoic chamber. The receiver unit consists of a duplex filter, three Rx filters and three amplifiers. The Rx filters have at least 60 dB Tx signal attenuation each and two of them are placed outside the chamber so that any possible. Tx signal leakage from cables is filtered out. The PIM analyzer is used both as a high-power signal source and in monitoring the reverse PIM signal level.

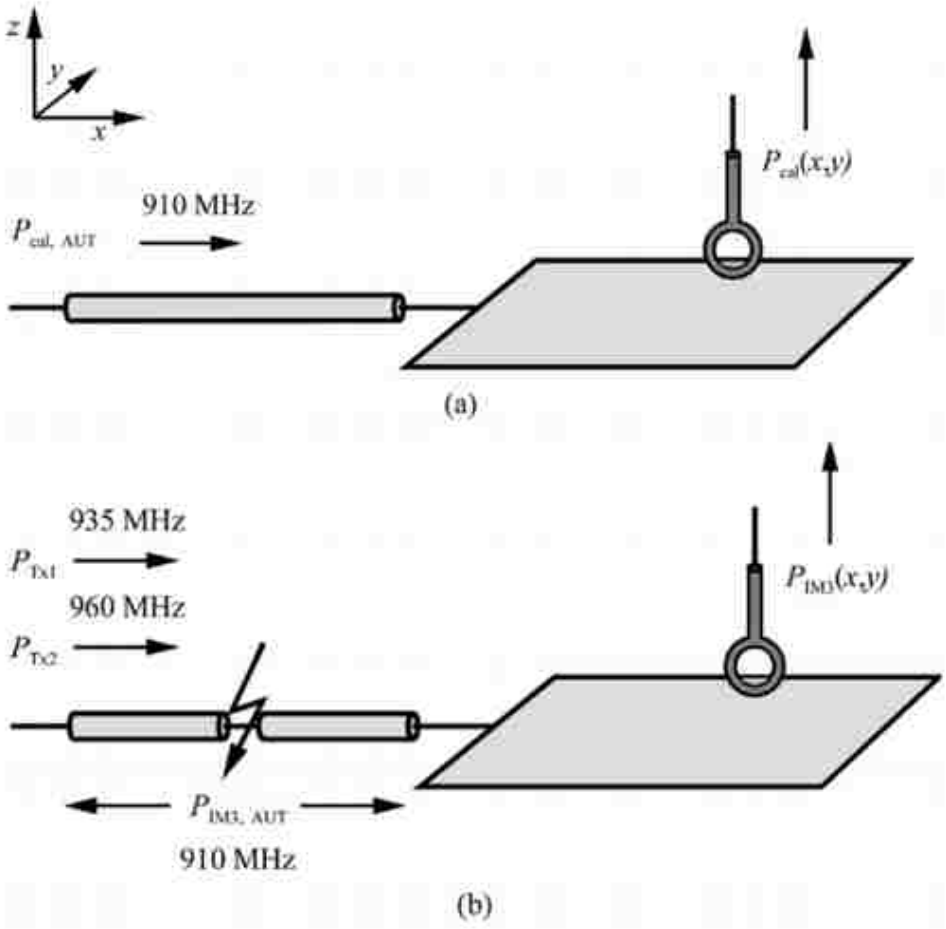

Figure 1.2. Normalization of the PIM near-field measurement [28].

The PIM signal is picked up by the near-field probe, then filtered and amplified by the receiver unit. The duplex filter in the receiver is an essential component in terminating the Tx signals. Otherwise, there would be a standing wave in the probe cable, which would lead to unpredictable PIM distortion. A vector network analyzer (VNA) is

used as the detector. By using coherent detection, the phase of the PIM signal can be measured and the sensitivity of the measurement is improved. The reference signal for the VNA is generated in the reference signal unit, which includes a mixer, amplifiers, filters, and RF switches. A Tx signal sample is taken with a low-PIM 53 dB coupler. The reference signal unit is also used to inject the calibration signal to the AUT. Both the stepping motors and the VNA are controlled by a computer. The PIM scanner operates in the GSM900 frequency band and its scanning range is 1.0 x 0.3 m.

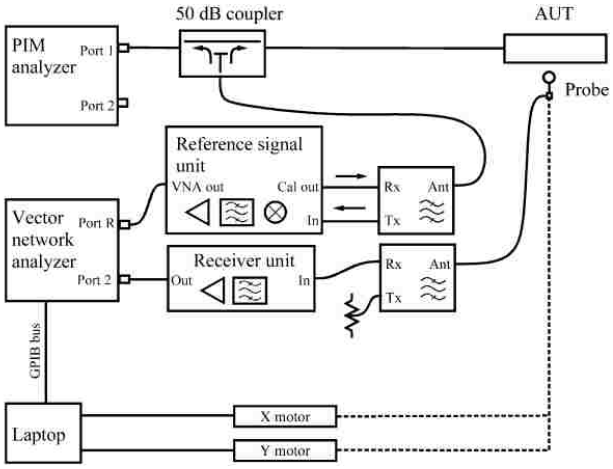

Figure 1.3. Block diagram of the PIM near-field measurement equipment [28].

The PIM near-field scanner can be used to localize PIM sources in an open transmission line and to identify faulty elements in antenna arrays. The implementation of the scanner is relatively straightforward to find the existing of PIM equipment. The construction of the probes is the most critical part in the PIM scanner development [28].

1.6. NEAR-FIELD SCANNING EXPERIMENT

Near-field probing was verified with a duplexer and a dipole probe. A measurement set-up is shown in Figure 1.4. The RF port of the PIM tester was connected to the input port of the antenna. Two transmitted signals come from PIM tester to antenna. Without the PIM source the PIM level was below -130 dBm in an anechoic chamber. When the transmitted signal frequencies were 1945 MHz and 1990 MHz, the

IM3 frequency was 1900 MHz. The transmitted signals were filtered by the duplexer which worked as a band pass filter with a passband between 1850 MHz and 1910 MHz. Though the frequency response of this duplexer was important, the more important factor was the PIM response. If the probe and the filter become a PIM source, the result of the spectrum analyzer was not guaranteed to be a true PIM power. Kaelus provided the duplexer which has low PIM characteristics. Two SAW band pass filters were connected to the duplexer in a series to reduce the transmitted signal power [33]. The center frequency of the spectrum analyzer was set to 1900 MHz which was the PIM frequency, the span was set to 2 kHz, and the resolution bandwidth was set to 20 Hz.

In order to measure the PIM level more stably, a simple supporting structure for the dipole antenna probe was made. A dipole probe shifted in space 3 cm in steps from #1 to #37 test points and maintained the same distance from the antenna.

Table 1.2 shows the measurement results of the first case of near-field probing. 1900 MHz frequency power levels were measured in the spectrum analyzer. The peak power levels near positions #6 and #7 have maximum value relative to other positions, which corresponds to the location of actual PIM source. Assuming the PIM source is constant with time, the PIM source could be located in this way with near-field probing. However, if the PIM level is time varying and is not stable with time it becomes difficult to find out the location of PIM source.

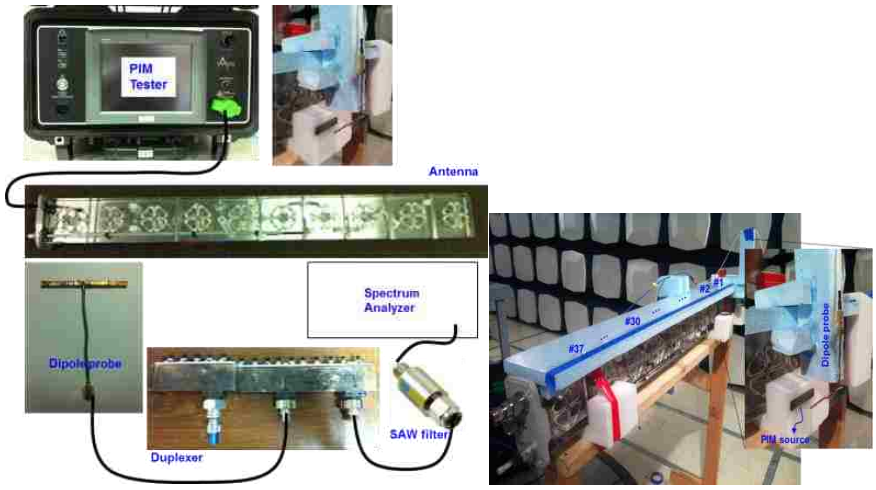

(a) (b)

Figure 1.4. Measurement set-up for near-field scanning.

Table 1.2. Near-field scanning when the PIM source existed on #7 in front of the base station antenna

Position #	Power level [dBm]	Position #	Power level [dBm]	Position #	Power level [dBm]	Position #	Power level [dBm]
#1	-71	#11	-66	#21	-81	#31	-82
#2	-61	#12	-63	#22	-73	#32	-83
#3	-59	#13	-64	#23	-70	#33	-82
#4	-56	#14	-66	#24	-70	#34	-81
#5	-49	#15	-67	#25	-73	#35	-80
#6	-44	#16	-67	#26	-72	#36	-80
#7	-45	#17	-69	#27	-73	#37	-82
#8	-51	#18	-74	#28	-75		
#9	-58	#19	-78	#29	-78		
#10	-67	#20	-79	#30	-79		

2. VIBRATION MODULATION METHOD

2.1. METHOD DESCRIPTION

The purpose of the vibration method is to locate the PIM source on the DUT through acoustic vibration [14]. It is expected that when vibrating at PIM source in acoustic/ultrasonic frequency (hundreds of Hz to hundreds of kHz), the amplitude of the intermodulated signal (f_{IM}) would be modulated by the vibration frequency (for example, 500 Hz) (Figure 2.1). This means the intermodulated signal has an amplitude modulation of the vibration frequency (f_{vb}). If the vibration position is not a PIM source, the intermodulated signal f_{IM3} would not have the amplitude modulation of the vibration frequency (f_{vb}). Thus, by checking the signal spectrum of the vibration modulated signal, the PIM source location could be determined.

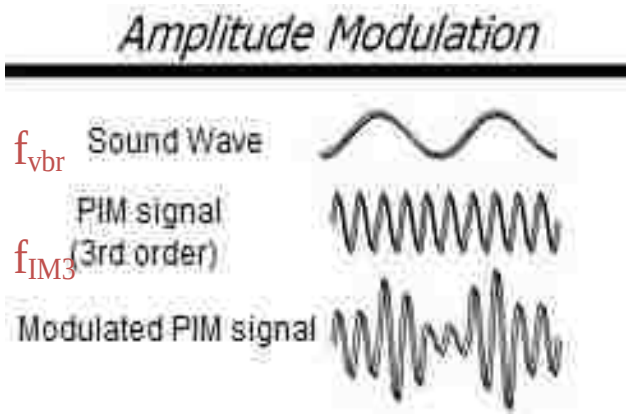

Figure 2.1. Amplitude modulation of modulated PIM signal when vibrating at PIM source.

As shown in Figure 2.2, the vibration method test set-up consists of several modules: the PIM analyzer, spectrum analyzer, oscilloscope, audio amplifier, and vibrating tool.

The PIM analyzer (Figure 2.3) generates two large signals (f1=1990 MHz, f2=1945 MHz), which go to the DUT. At the PIM source location on the DUT, the

modulated frequency f_{IM3}=1900 MHz would be generated by the intermodulation and reflected back to the PIM analyzer. Then, the 1900 MHz f_{IM3} would be filtered and go to the RF output port on the PIM analyzer.

A spectrum analyzer (Figure 2.4) with video output port on the back was used here. The RF output of the PIM analyzer was used as the input of the spectrum analyzer.

The intermodulated signal from the RF output port of the PIM analyzer was transferred to the spectrum analyzer input.

The parameters of the spectrum analyzer setting are shown below:

- Center frequency = $f_{IM3.}$ If the center frequency is not certain, the peak of the signal can be found by setting the span to 100 MHz.
- Span = 0. When span is zero, the envelope of the signal can be analyzed, which means the AM vibration signal can be picked out by a zero span.
- Resolution bandwidth (RBW), video bandwidth; 3 or 4 times of vibration frequency ($3\sim4*f_{vbr}$). With these settings, the amplitude envelope of f_{IM3} signal at the SA's video output port is obtainable. When the vibration of transducer operates at 500 Hz, the RBW is set to around 2 kHz.
- RF attenuation. In order to reduce the noise floor and gain the high signal-to-noise ratio, RF attenuation was set to 0 dB.

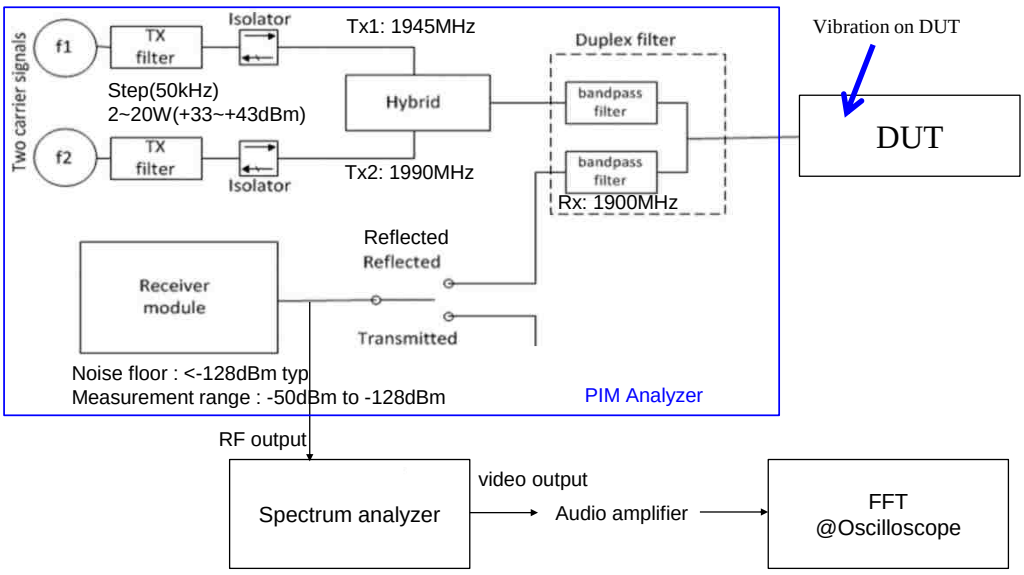

Figure 2.2. System diagram of vibration method.

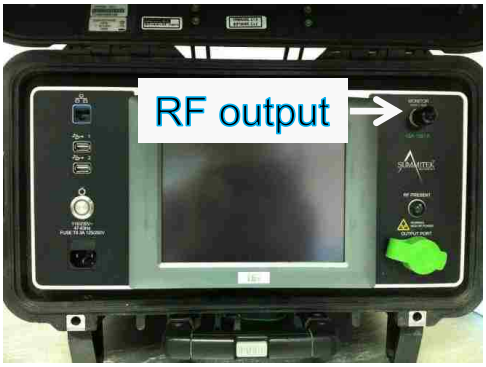

Figure 2.3. Kaelus PIM analyzer.

Figure 2.4. Rohde & Schwarz Spectrum Analyzer equipped with video output.

The video output port was connected to the oscilloscope input port and an audio amplifier was used to amplify the envelope signal strength. Because the vibrating frequency of the transducer was within the audio frequency, an audio amplifier (Figure 2.5) was used to detect the modulated spectrum more effectively in the oscilloscope [30]. It has a gain of approximately 20 to 30 and it also works as a low pass filter. Then, the oscilloscope processes the envelope signal to frequency domain through FFT.

The envelope was expected to have the frequency component of f_{vbr} when the PIM source was vibrated by the vibrating tool. When the vibration happened at other locations other than at the PIM source, the PIM source point was not affected by the

vibration; thus, the spectrum of f_{vbr} on the oscilloscope would not be observed at this time. By observing whether there was the spectrum of f_{vbr} on the oscilloscope, the PIM source location could be determined (Figure 2.6).

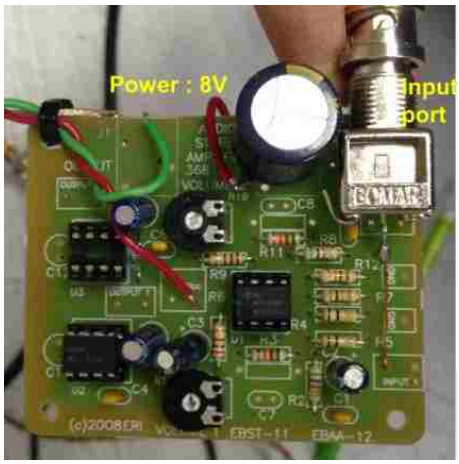

Figure 2.5. Audio amplifier for amplifying RF output of PIM tester.

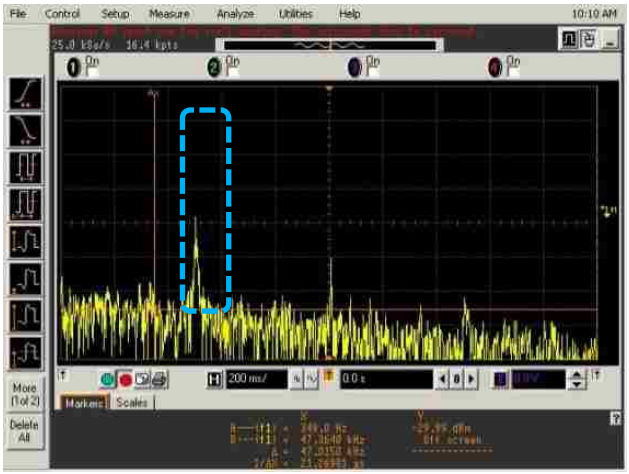

Figure 2.6. Vibrating at PIM source.

The method was first investigated on the loose connector set-up in order to validate the method. Different vibrating tools were tested and are summarized in the following sections. The vibration method was applied to base station antenna and the results are shown in the later sections.

2.2. MEASUREMENT WITH LOOSE CONNECTORS

The measurement set-up is shown in Figure 2.7. Two pieces of coax cable were used here. One end of the cable was connected to the PIM analyzer's RF output and the other end was connected to the Kaelus Low PIM 50 Ohm load (Figure 2.8). The connection between the two cables was intentionally loosened in order to create a PIM source.

Four different kinds of vibrating tools were investigated because different vibrating methods may have different vibration frequencies, displacement, power, etc. It is important to learn the characteristics, advantages, and disadvantages of each vibrating method.

There are two vibrating positions (Figure 2.9) in this measurement set-up: 1) at the loose connector (PIM source) and 2) at 50 cm away from the PIM source on the cable.

Figure 2.7. Measurement set-up of the vibration method.

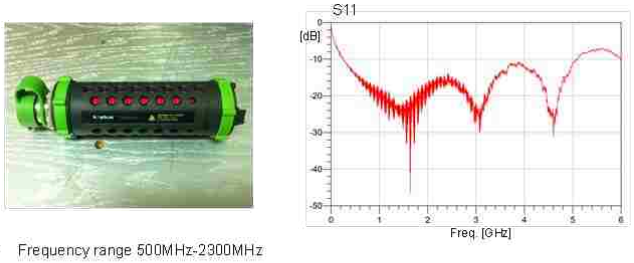

- Frequency range 500MHz-2300MHz
- RF impedance = 50 ohms
- PIM < -107dBm (2x43dBm carriers), typically < -115 dBm
- 40W, 3 mins (with 1:3 on/off ratio)
- Connector : 7/16 female
- Dimension (L x D) : 190 x 60mm (7.48 x 2.36in)

Figure 2.8. Kaelus Low PIM 50 Ohm load and its parameters.

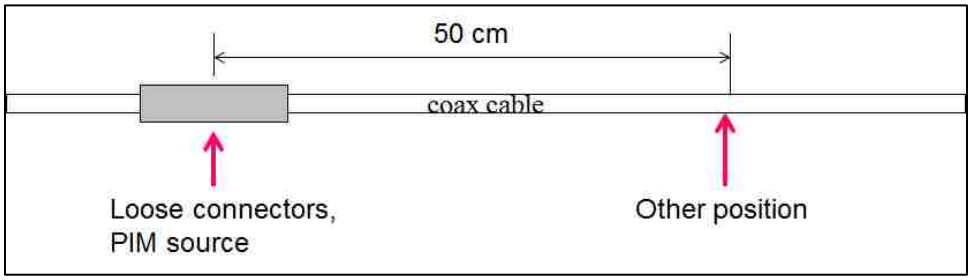

Figure 2.9. Two vibration locations on the DUT (two piece of coax cable).

2.2.1. DC Motor. A DC motor was investigated as the vibrating tool first. Figure 2.10 shows the parameters of the DC motor. The DC motor has a rather low operation frequency and large displacement compared to the speakers or ultrasonic transducers in the later section. The motor was mounted to the loose connectors as shown in Figure 2.11.

2.2.2. Buzzer. A Buzzer (Figure 2.12) transducer type "102-1153-ND CEM 1203" was used for the second vibrating tool at three different frequencies: 0.998 KHz, 1.698 KHz, and 2.001 KHz. The amplitude varies with. In Figure 2.12 below, the photo of transducer and its frequency behavior are shown. The buzzer is mounted to the measurement set-up as shown in Figure 2.13. The buzzer has a high operation frequency and small displacement.

2.2.3. Audio Speaker. Two types of speakers (Figure 2.14) were used in the third experiment. The vibration of a speaker comes from the front, and it is difficult to transfer the vibration to the locations on the DUT. Thus, a screw was attached to the front side of a speaker as shown in Figure 2.14 (c) and (d) to deliver the vibration more effectively. A plastic rod might be a better medium than a metal screw for eliminating the interference caused by metal contact between the vibration source (speaker) and the DUT. A signal generator (Figure 2.15) was used to drive the speaker to the desired frequency. The output of a signal generator is a sinusoidal wave and has a 20 V peak amplitude. The operation frequencies of the speakers are 200 Hz-3 kHz.

2.2.4. Ultrasonic Transducer. The fourth vibrating tool was an ultrasonic transducer (Figure 2.16). It has the highest vibration frequency and smallest displacement. Since it consumes rather large power (50 W), a power amplifier was

needed to generate enough power. The signal generator was tuned to the transducer's resonant frequency around 28 kHz in order to generate maximum vibration.

45000RPM 1.5V-9V DC 222A Rated Current Vibrating Vibration Micro Motor
Operation frequency : ~100Hz (6000RPM), large displacement

Figure 2.10. DC motor and its parameters.

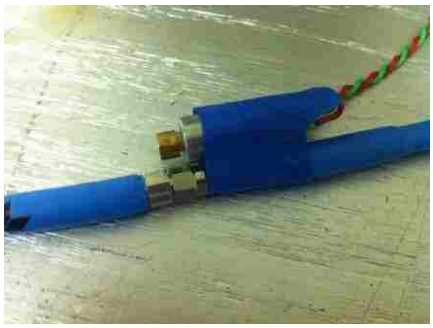

Figure 2.11. Illustration on how the DC motor was mounted to the cable.

Specifications

Rated voltage	3.5 Vo-p	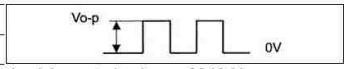
Operating voltage	3.0 - 5.0 Vo-p	
Mean current	35 mA max.	Applying rated voltage, 2048 Hz square wave, ½ duty
Coil resistance	42 ±6.3 Ω	
Sound output	Min. 85 (Typical 95) dBA	Distance at 10cm (A-weight free air). Applying rated voltage of 2048 Hz, square wave, 1/2 duty.
Rated frequency	2,048 Hz	
Operating temperature	-20 ~ +60° C	
Storage temperature	-30 ~ +70° C	
Dimensions	ø12.0 x H8.5 mm	See attached drawing
Weight	1.4 g	
Material	PPO (Black)	
Terminal	Pin type (AU Plating)	See attached drawing
RoHS	yes	

Figure 2.12. The buzzer and its parameters

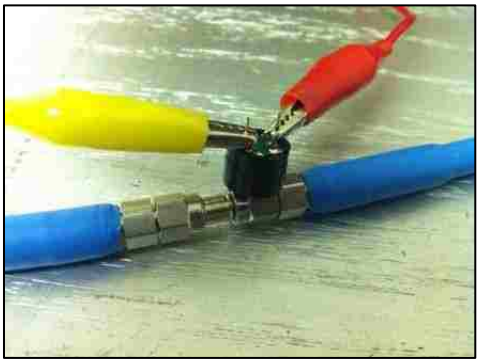

Figure 2.13. Illustration on how the buzzer was mounted to the cable.

Figure 2.14. Two types of speakers that were used in the measurement.
(a) BDM8760F 8Ohm, (b) GENTO SP99023A 4Ohm.

Figure 2.15. Signal generator to drive the speaker to operation frequency.

The power amplifier was based on power opamp MP118 (Figure 2.17 and Figure 2.18) from Apex Microtechnology [31]. The supply voltages of +60 V, -60 V are used for generating enough power. As shown in Figure 2.17, two power supplies are used for both +60 V and -60 V. The input signal of the power amplifier is generated by a signal generator and is set to 2 V peak-to-peak amplitude.

Operating Frequency	28kHz
Capacitance	3.8nF
Impedance	50 max.
Mechanical Q (Qm1)	800 min.
Power	50 watts
Coupling Factor (kp)	55% min.
Major OD	45mm
Overall Length	80mm
Model	DAT-28

Figure 2.16. Ultrasonic transducer and its parameters.

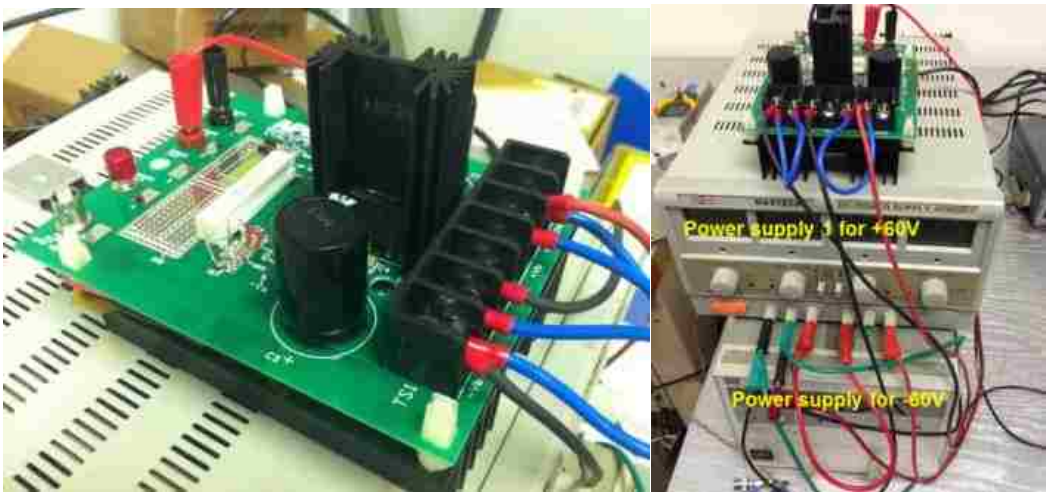

Figure 2.17. Apex MP118 evaluation kit to drive the transducer.

Figure 2.18. A holder was used to support the transducer.

2.3. MEASUREMENT RESULTS AND ANALYSIS WITH LOOSE CONNECTORS

All four vibration tools were tested in this experiment and for each vibration tool, vibration at the loose connector and at another position was measured. The table below summarized the results of all the tests. "Vibration modulated" means that the vibration frequency f_{vbr} was observed on the oscilloscope and "Not found" means that the vibration frequency f_{vbr} could not been seen on the oscilloscope.

As shown in Table 2.1, when using a DC motor as the vibrating tool, the modulated vibration signal was observed for both positions. This means that the DC motor's displacement was so large that the entire structure vibrated and thus resulted in amplitude modulation on the 1900 MHz PIM source signal.

As for the results of the buzzer, it was rather hard to observe a modulated signal even when it vibrated at the loose connector because the buzzer was difficult to mount steadily to the DUT structure since it was too small.

The results of the speakers varied according to the operation frequencies. The displacement was smaller as the operation frequency increased. At low frequency (for example, 200-300 Hz), the displacement was large enough to vibrate the entire structure, thus the result was similar to those of DC motor. When the frequency was high (for example, 600Hz-1kHz), the displacement was small and the vibration only affected a

small section of the structure. When vibrating at the PIM source, the modulated vibration signal was observable on the oscilloscope; while the vibration was at other positions, the modulated vibration signal couldn't be observed. Thus, the PIM source was able to be located.

Table 2.1. Comparison of different vibration sources

Vibration Source	Characteristics	Position	
		Loose connector (PIM source)	Other position (50 cm from PIM source)
DC motor	Low frequency (tens of Hz-200 Hz) Large displacement Easy to couple to cable and connector using tape	Vibration modulated	Vibration modulated
Buzzer	1-2 kHz Small displacement Difficult to make vibration couple	Sometimes found	Sometimes or not found
Speaker	Hundreds of Hz-kHz Using screw or ceramic rod to deliver vibration A holder was used	Vibration modulated	Dependent on the displacement (frequency) - vibration frequency could be observed when it was low
Ultrasonic transducer	28 kHz A holder was used	Sometimes found	Not found

The results of the ultrasonic transducer were similar to the results of the speaker with higher operation frequencies. However, the displacement was so small that the ultrasonic transducer had to be carefully placed at the PIM source in order to see the modulated vibration signal.

In conclusion, DC motors and buzzers are not suitable for the vibration method. When the operation frequency is high, the speaker could be used to locate the PIM source. The ultrasonic transducer is another choice; however, its displacement is rather weak and the ultrasonic transducer has to be placed carefully at the PIM source in order to get the modulated vibration signal.

2.4. MEASUREMENT ON BASE STATION ANTENNA

After the loose connector tests, the vibration modulation method was applied to a real base station antenna to investigate its potential and limitations. The base station antenna used in this set-up is Huawei Model A19451811. Figure 2.19, Figure 2.20, Figure 2.21, and Figure 2.22 are the antenna's electrical properties and physical dimensions.

2.5. ANTENNA PIM LEVEL MEASUREMENT

Before performing the vibration method experiments, the PIM level of the antenna itself was measured (Figure 2.23). The antenna was placed inside an anechoic chamber to remove reflections and potential PIM sources from surroundings. A low PIM cable from Kaelus was used in the measurement to avoid potential PIM sources from cabling (connectors, etc.).

The antenna has the typical PIM level of -131 dBm, which is a very good result. The standard for PIM requires a pass level of -97 dBm/-140 dBc.

The antenna's S11 and S21 were also measured, the S-parameters indicate that the antenna works fine in the designated frequency range of 1710 MHz-2200 MHz.

2.5.1. Ferrite Debris As PIM Source. A small piece of ferrite was placed at different locations on the antenna to create a PIM source. The antenna elements in the array were numbered as 1 to 10 from top to bottom, as shown in Figure 2.24. For each dipole antenna, the ferrite was placed at the center of it, as shown in Figure 2.25.

Electrical Properties													
Frequency range (MHz)	1710 - 2200												
	1710 - 1880			1850 - 1990			1920 - 2170			2170 - 2200			
Polarization	+45°, -45°												
Electrical downtilt (°)	0 - 10, continuously adjustable												
Gain (dBi)	0°	5°	10°	0°	5°	10°	0°	5°	10°	0°	5°	10°	
	17.2	17.6	17.4	17.7	18.0	17.7	18.0	18.1	17.9	18.0	18.2	17.9	
Side lobe suppression for first side lobe above main beam (Typ.) (dB)	0°	5°	10°	0°	5°	10°	0°	5°	10°	0°	5°	10°	
	20	16	18	20	20	18	18	17	16	18	18	16	
Horizontal 3dB beam width (°)	67			64			61			60			
Vertical 3dB beam width (°)	7.5			7.0			6.7			6.2			
VSWR	< 1.5												
Isolation between ports (dB)	≥ 30												
Front to back ratio, copolar (dB)	Typ. 30												
Cross polar ratio (dB) 0°	Typ. 22												
Cross polar ratio (dB) ±60°	Typ. 10												
Max. power per input (W)	300 (at 50°C ambient temperature)												
Intermodulation IM3 (dBc)	≤ -153 (2 x 43 dBm carrier)												
Squint (°)	Avg. 1.2												
Tracking (dB)	Avg. 1.2 (within 10dB HBW)												
Impedance (Ω)	50												
Grounding	DC Ground												

Figure 2.19. Electrical properties of the base station antenna.

Mechanical Properties	
Antenna dimensions (H x W x D) (mm)	1311 x 155 x 89
Packing dimensions (H x W x D) (mm)	1635 x 195 x 160
Antenna weight (kg)	6.2
Clamps weight (kg)	2.0 (2 units)
Antenna packing weight (kg)	11.2 (Included clamps)
Mast diameter supported (mm)	38 - 115
Radome material	Fiberglass
Radome colour	Light grey
Operational temperature (°C)	-55 .. +65
Wind load (N)	Frontal: 315 (at 150 km/h) Lateral: 155 (at 150 km/h) Rear side: 360 (at 150 km/h)
Max. operational wind speed (km/h)	150
Survival wind speed (km/h)	200
Connector	2 x 7/16 DIN Female
Connector position	Bottom

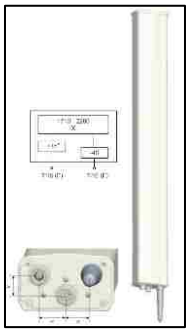

Figure 2.20. Antenna dimensions and mechanical properties.

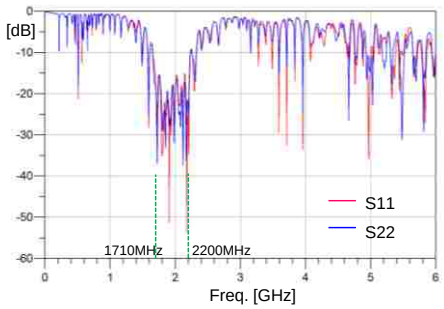

Figure 2.21. Reflection (S11, S22)

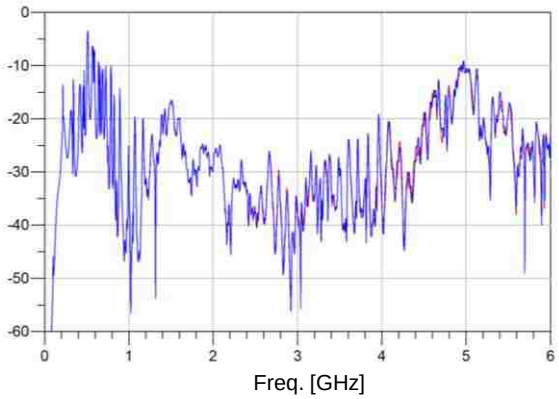

Figure 2.22. Isolation (S12, S21).

Figure 2.23. Antenna PIM level measurement set-up.

The measurement results have been summarized into Table 2.2. From the table above, it was observed that the ferrite debris had a strong PIM effect only at the central antenna elements (fifth and sixth antenna) on the array.

Figure 2.24. Antenna set-up.

Figure 2.25. Small ferrite piece attached to the center of dipole antenna.

Table 2.2. PIM level of different ferrite placement

Place	Peak PIM level [dBm]
Center ground plate	-130.4
Second dipole at front	-132.5
Third dipole at front	-132.6
Fourth dipole at front	-132.5
Fifth dipole at front	-111.0, -99.6
Sixth dipole at front	-104.2
Eighth dipole at front	-130.1
Ninth dipole at front	-128.8
Electric downtilt at back	-129.9
Ground plate at back	-132.7
Splitter at back	-131.9
Signal lines at back	-131.7, -132.3, -130.7

2.5.2. Investigation of PIM Problem Caused By Vibration. One of the main concerns of the vibration method is that the vibration itself may cause a PIM effect which would result in a false PIM location. Thus, it is necessary to investigate the vibration-caused PIM effect before performing the vibration method.

In this section, a DC motor was used to generate a strong vibration (Figure 2.26). The DC motor was attached to different places on the antenna. The PIM level was around -130 dBm for all these measurements. Even when the vibration is as strong as the one generated by the DC motor, it would not cause a PIM effect. Thus, the vibration method is ready to apply to the antenna array.

2.6. VIBRATION METHOD ON BASE STATION ANTENNA ARRAY

There are three types of PIM sources in this measurement: ferrite debris (Figure 2.27), metal debris (Figure 2.28), and a bad soldering joint (Figure 2.29). When these PIM sources were applied to the solder joint, a significant rise in PIM level could be observed.

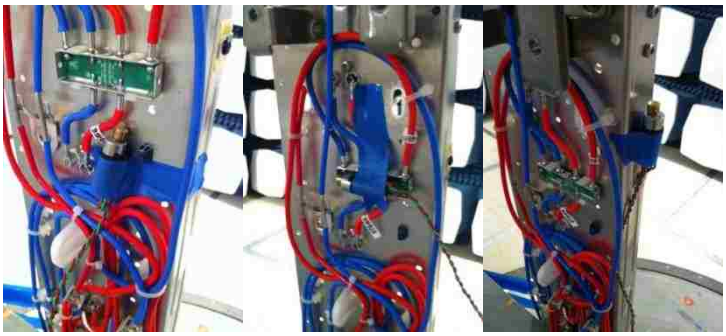

Figure 2.26. DC motor was placed to different places on the base station antenna.

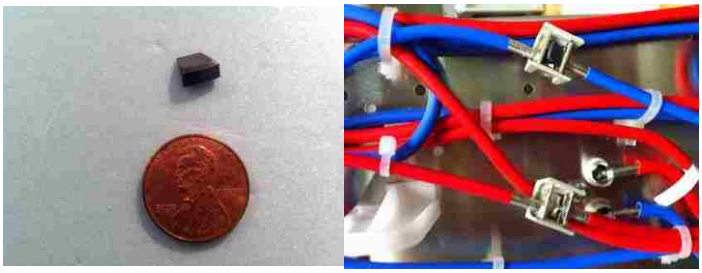

Figure 2.27. PIM source I: ferrite debris.

Figure 2.28. PIM source II: metal debris.

Two potential PIM source locations were investigated: the solder joint (Figure 2.30) and the E-downtilt (phase shifter) (Figure 2.31).

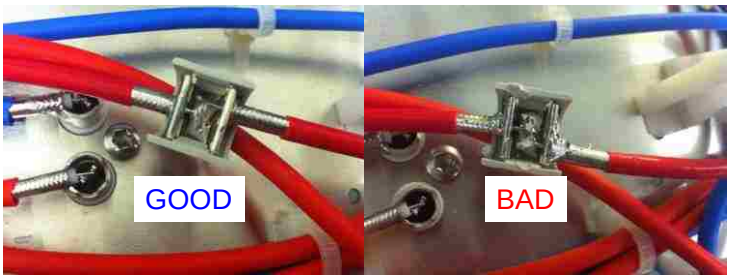

Figure 2.29. PIM source III: bad soldering.

Two types of vibration tools were used here: the audio speaker (Figure 2.32) and the ultrasonic transducer (Figure 2.33).

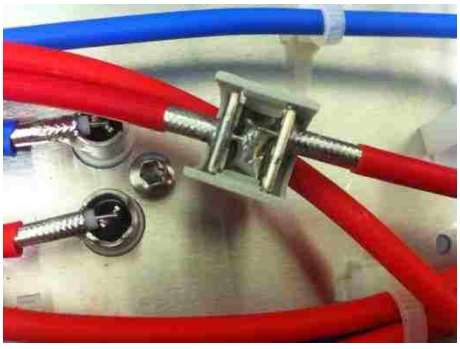

Figure 2.30. Potential PIM source location I: Solder joint.

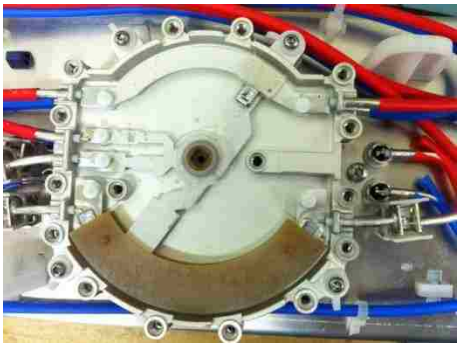

Figure 2.31. Potential PIM source location II: E-downtilt (phase shifter).

Figure 2.32. Vibration tool I: speaker.

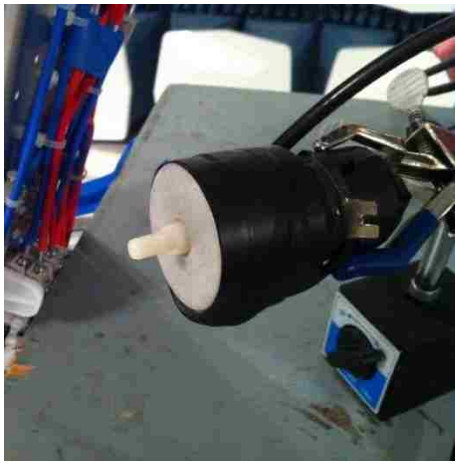

Figure 2.33. Vibration tool II: ultrasonic transducer.

2.7. MEASUREMENT RESULTS AND ANALYSIS OF BASE STATION ANTENNA

The base station antenna faced the wall in the anechoic chamber as shown in Figure 2.24. After some experiments, a supporting frame for the antenna was made. If the floor was not composed of a series of wedges, the antenna had to be carefully placed to avoid ..falling to the floor. One of the input ports of the antenna was connected to the input port of the PIM tester. In this experiment, the other port of the antenna was floating. The RF output port of the PIM tester was connected to the input port of the spectrum analyzer and the video output of the spectrum analyzer was connected to the audio amplifier. The amplified signal was connected to the oscilloscope and the FFT magnitude of the input signal was observed by using the FFT function. The center frequency of FFT function was set to around the vibration frequency. For example, when the 500 Hz~1 kHz vibration was used, the center frequency of FFT was set to 600 Hz and the step was set to 100 Hz.

The measurement results of the vibration method on the base station antenna array have been summarized to following tables. Table 2.3 shows the bad soldering case. Bad soldering was not the mechanical issue, so there was no modulation in FFT even when the vibration was delivered to the solder joint itself. The vibration method seems more effective for locating the mechanical PIM sources.

Table 2.3. Case III – Bad solder joint

Vibration at bad solder joint	Modulated signal in FFT
500 Hz	not found
600 Hz	not found
700 Hz	not found
1 kHz	not found

Table 2.4 shows the result when the ferrite debris was used as the PIM source. When the ferrite debris was attached to one of the solder joints on the antenna, the PIM level was in the range of -70 to -87 dBm. In order to confirm that the vibration method was effective, the vibration was first delivered to the solder joint that had a ferrite piece then the other position, such as the ground plane of the antenna, was vibrated.

In this case, 700 Hz of vibration was appropriate. When the vibration was close to the PIM source the modulated signal could be found, and when the vibration was far from the PIM source there was no modulated signal. This means the PIM source could be determined by using a 700 Hz vibration of the transducer.

Table 2.4. PIM source - Ferrite piece

PIM source	Ferrite piece attached to the solder joint	
Vibration	At solder joint with ferrite piece	At other position (antenna ground)
500 Hz	PIM: -86.5 dBm, Amplitude modulated	PIM: -69.2 dBm Amplitude modulated
600 Hz	PIM: -87.1 dBm, Amplitude modulated	PIM: -70.8 dBm Amplitude modulated
700 Hz	PIM: -84.7 dBm, Amplitude modulated	PIM: -70.9 dBm No modulation
1 kHz	PIM: -68.2 dBm, No modulation	No modulation
2 kHz	PIM: -70.6 dBm, No modulation	No modulation

Metal debris could also be a PIM source. A small amount of metal debris was attached to the solder joint which resulted in an increase of the PIM level. The vibration method to locate the PIM source worked with 300 Hz, 500Hz, 600 Hz, and 700 Hz vibrating frequencies. In the case of the 1 kHz vibration, the displacement of the vibration was not enough to generate a modulated signal even when the source position was vibrated as shown in Table 2.5. The last row of Table 2.5 shows the result of when the ultrasonic transducer was used.

Table 2.5. PIM source - Metal debris at the solder joint

PIM source	Metal debris at solder joint	
Vibration	At solder joint with metal debris	At other position (antenna ground)
300 Hz	PIM:-122.6 dBm Amplitude modulated	PIM:-109.6 dBm No modulation
500 Hz	PIM:-108.0 dBm Amplitude modulated	PIM:-86.7 dBm No modulation
600 Hz	Amplitude modulated	PIM:-88 dBm No modulation
700 Hz	Amplitude modulated	PIM:-91.2 dBm No modulation
1 kHz	Sometimes modulated	PIM: -79.5 dBm No modulation
28 kHz (ultrasonic)	-91.2 dBm Amplitude modulated	-121.2 dBm No modulation

The vibration of the ultrasonic transducer close to the PIM source (metal debris at solder joint) could induce the amplitude modulation; while the vibration becomes far from the PIM source, there is no modulation. This means the vibration method for locating a PIM source works with the ultrasonic transducer as well.

E-downtilt (phase shifter) was also a potential area to be a PIM source. When the metal debris was placed inside of the E-downtilt after opening the cover, the PIM level increased. By using the ultrasonic transducer, the PIM source position could be found as shown in the Table 2.6.

In conclusion, all results and analysis show that the vibration method was able to locate the PIM source on a real base station antenna array. A 700 Hz vibration generated by a speaker or ultrasonic transducer was a better vibration tool for the vibration method. Further investigation needs to be conducted in order to find why the vibration method failed when bad soldering was the PIM source.

Table 2.6. PIM source - Metal debris in E-downtilt

PIM source	Metal debris in E-downtilt	
Vibration	At E-downtilt (phase shifter)	At other position (antenna ground)
28 kHz	-79.4 dBm Amplitude modulated	-80.5 dBm No modulation

3. PIM SOURCE IDENTIFICATION SYSTEM

Since the effectiveness of the vibration method for PIM source identification was proven in previous sections, designing a PIM source identification system became our interest. The system consisted of two subsystems, a PIM receiver and a PIM vibrator.

The PIM receiver takes in the RF signal from the PIM analyzer. The PIM analyzer's RF signal consists of the PIM signal along with other frequency components such as two base frequencies, ambient RF spectrum, etc. The main purpose of the PIM receiver is to increase the signal-to-noise ratio (SNR) of the PIM analyzer's RF signal. It also downmixes the RF signal to a proper frequency for filtering and analysis. The PIM vibrator subsystem provides the vibration source for the vibration modulation method. It consists of an ultrasonic transducer, ultrasonic driver, and signal source. A glass tip was made for better vibration delivery.

3.1. PIM RECEIVER

The schematic of the PIM receiver is shown in Figure 3.1. The PIM receiver subsystem consists of the following components: a PGA103+ LNA module, a cellular SAW filter bank module, a 2-way splitter module, two MAX2870 frequency synthesizer modules, two ADL5801 modules, a 120 kHz@433.92 MHz SAW filter module, two 80 MHz low-pass filters (LPF), an ADL5611 variable gain amplifier, a variable bandwidth filter bank, a Mini-Circuits 40 dB high gain amplifier, a 3-way splitter module, a detector module, an audio amplifier module, and a touchscreen control panel.

The purpose of the PIM receiver subsystem is to increase the SNR of the PIM analyzer's RF signal. To achieve this goal, an LNA module was placed at the first stage of the PIM receiver subsystem. The LNA minimized the noise floor rise due to amplification in the system. Then, a SAW filter bank was added next to the LNA module to filter out only the PIM signal component. The SAW filters were selected specifically so that the desired PIM signal would fall into one of their pass bands. Further amplification and filtering was needed to purify the PIM signal, and the equivalent bandwidth of the band-pass filter was required by the sponsor. Thus, there are two stages of downmixing after the cellular SAW filter bank to accomplish these demands. The IF

frequency AM signal then passed to the detector board; there are two envelope detection methods to get the envelope of the AM signal.

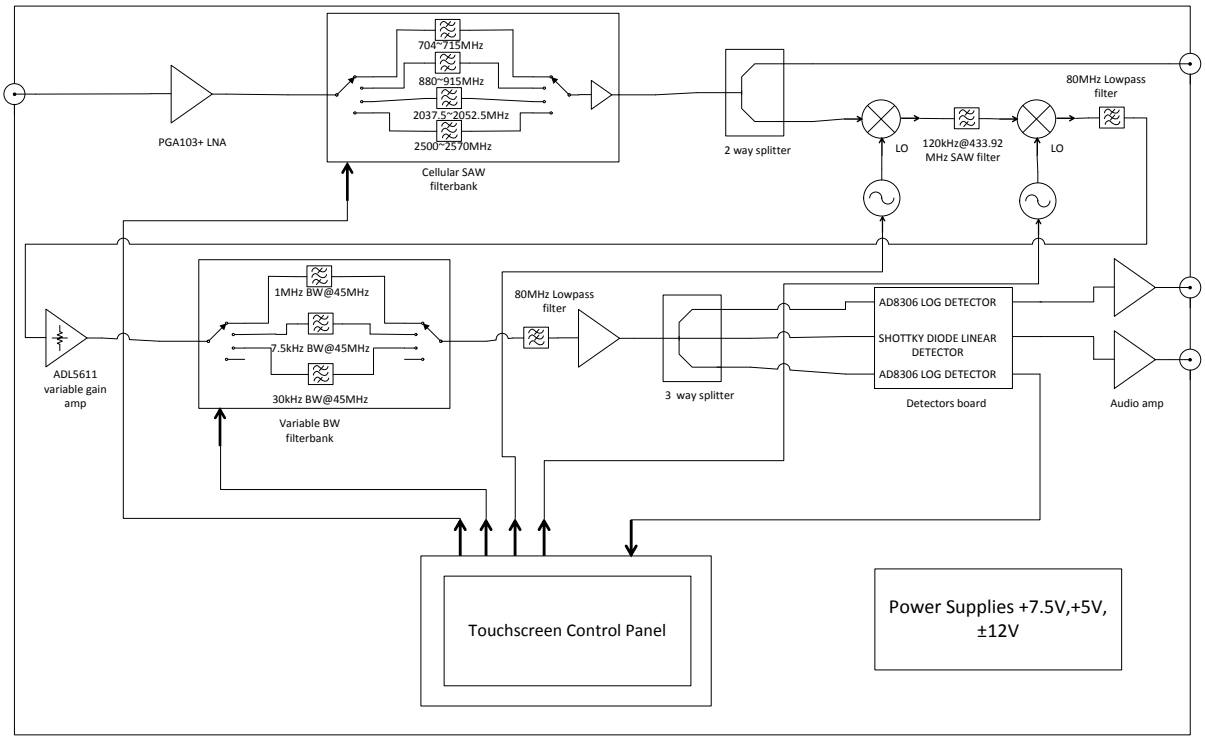

Figure 3.1. PIM Receiver system schematic.

3.1.1. PGA103+ LNA Module. In the real PIM test environment, the IM3 signal (for example, 1900 MHz) coupled with both base frequency signals (for example, 1945 MHz and 1990 MHz). The base frequency signal was still large enough to saturate the first stage amplifiers; thus, it's necessary to select the amplifiers for the first stage that have a low noise figure and high third order intercept (OIP3) value.

The selected PGA-103+ (Figure 3.2) from Mini-Circuits has a low noise figure (0.9 dB at 2 GHz) and very high OIP3 (45 dBm at 2 GHz); however, its gain changes with frequency rapidly. A compensation circuit was built after each amplifier and contained three PGA103+ ICs in a series to have enough gain. The compensation circuit (Figure 3.3) attenuated the gain in the low frequency, while in the high frequency the

circuit had less attenuation. The resistor values were selected so that the input and output impedance was 50 Ohm and the component values were optimized in ADS.

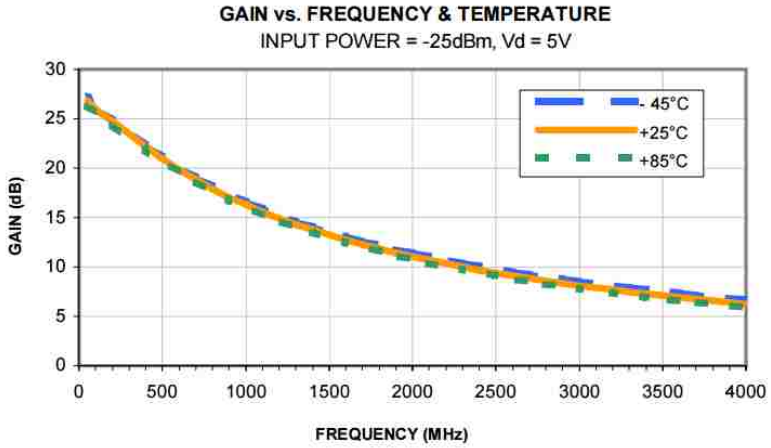

Figure 3.2. PGA103+ gain vs. frequency.

The measurement results show that this board (Figure 3.4) has a 39 dB gain at 433.92 MHz, a 30 dB gain at 900 MHz, and a 26 dB gain at 1.8 GHz (Figure 3.5).

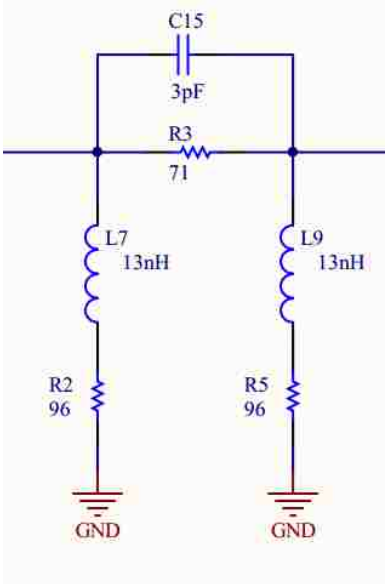

Figure 3.3. Gain compensation circuit.

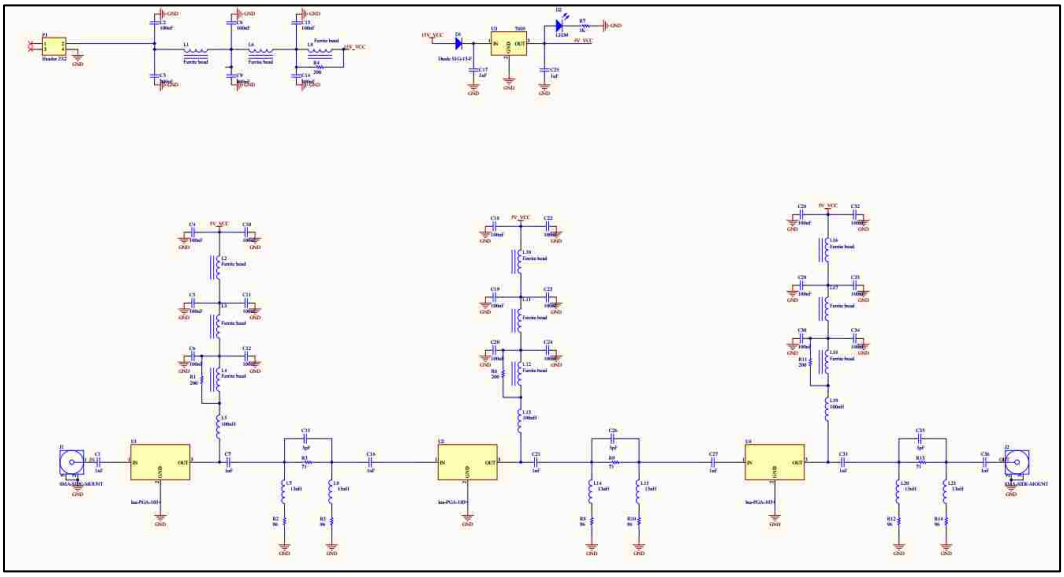

Figure 3.4. Schematic of first stage amplifier.

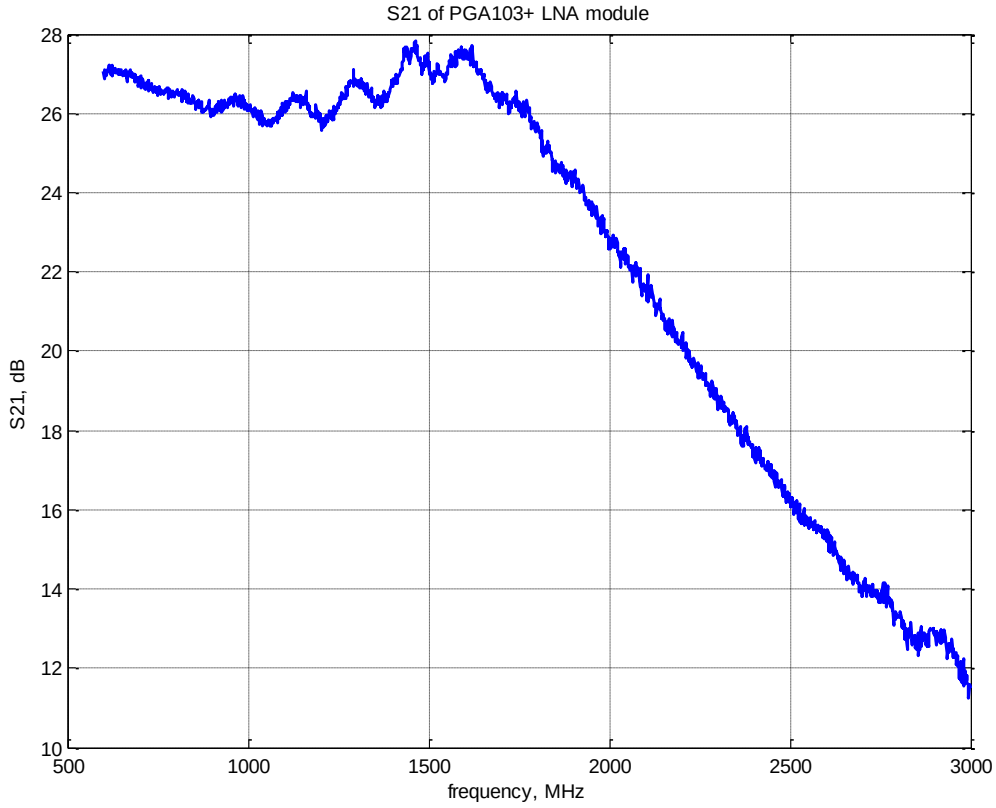

Figure 3.5. S21 measurement results for the first stage amplifier with external 40dB attenuation.

3.1.2. SAW Filter Bank. Four SAW filters were selected based on the sponsor's requirements. Table 3.1 shows the 4 cellular bands that were required by the sponsor.

Figure 3.6 shows the schematic of the circuit. RF relays were used to switch between different SAW filters. Since the system is controlled by a touchscreen panel, a relay driver was selected to drive the RF relays. There is also attenuation on the SAW filter, so an ADL5611 amplifier was added at the last stage to boost the signal power. Figure 3.7 shows the measured S21 of the cellular SAW filter board.

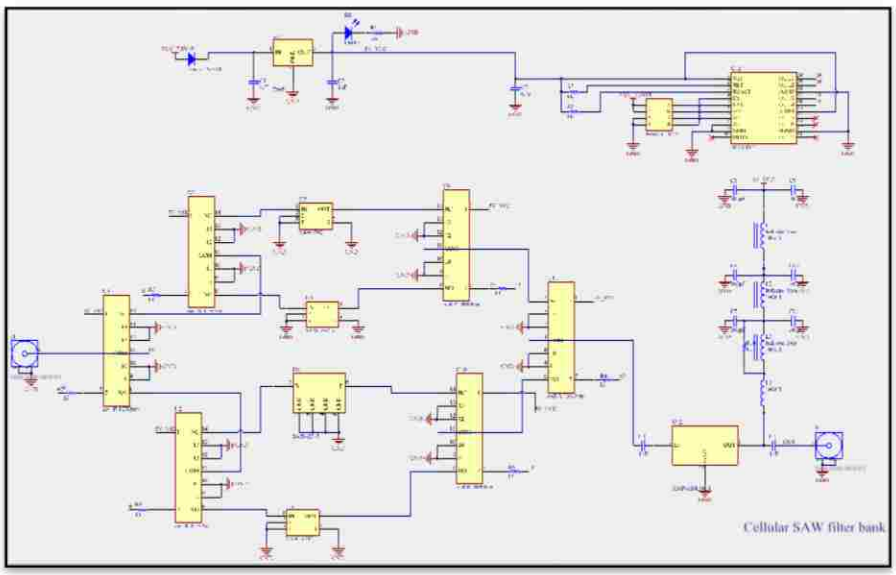

Figure 3.6. Cellular SAW filter bank circuit diagram.

3.1.3. Mixer. The mixer IC used was an ADL5801. It operated in single-ended mode in a very wide range (LO 200 MHz to 6 GHz). It had a conversion gain of 1.8 dB and the input IP3 was 28.5 dBm (Figure 3.8). Table 3.2 and Table 3.3 are the measured mixer performance at different frequencies.

3.1.4. MAX2870 Frequency Synthesizer. A MAX2870 frequency synthesizer (Figure 3.9) was selected as the LO of the mixers. The MAX2870 was programmed to generate frequencies from 23.5 MHz to 6000 MHz. A control code was developed in the touchscreen panel to generate the LO frequencies needed by the mixers.

Table 3.1. SAW filters for different cellular bands

Standard	PIM frequency
LTE700	704-850 MHz
EGSM900	880-915 MHz
UMTS2100	2050-2060 MHz
LTE2600	2550-2570 MHz

3.1.5. 433.92 MHz SAW Filter. Figure 3.10 is the schematic of 433MHz SAW filter. This SAW filter has passband as narrow as 120kHz. The measured S21 of this SAW filter board is shown in Figure 3.11, which indicates that the filter has about 3.1dBm insertion loss at 433.92MHz.

3.1.6. Variable Bandwidth Filter Bank. As required by the sponsor, a variable bandwidth filter bank was added to the system. The expected pass band bandwidth would be 2 kHz, 10 kHz for audio frequency, and 80kHz for ultrasonic frequency.

A thorough search for a source of narrow band bandpass filters was done and found that the desired filters have to be customized, which would have resulted in an unacceptable lead time. Thus, the final selection of the filters had to take the availability into consideration.

The ECS-75SMF crystal filters shown in Table 3.4 were selected for their appropriate bandwidth and availability; the 7.5 kHz and 30 kHz bandwidth were selected. Since the filters' center frequency was 45 MHz, and the stage before it was a 433.92 MHz SAW filter, a mixer was needed to downmix the input signal to this frequency.

Another 1 MHz bandwidth filter shown in Figure 3.12 was designed and simulated in ADS and then implemented on the PCB.

Since there was a 120 kHz bandwidth 433.92MHz SAW filter before this stage, it had a 120 kHz equivalent bandwidth when this filter was selected. The schematic is shown in Figure 3.13.

The measurement results (Figure 3.14) show that this board has tunable gain from 33dB to 61.2 dB. During the test it was discovered that the system total gain might not be enough for the linear detection method, thus, another gain block was added to system.

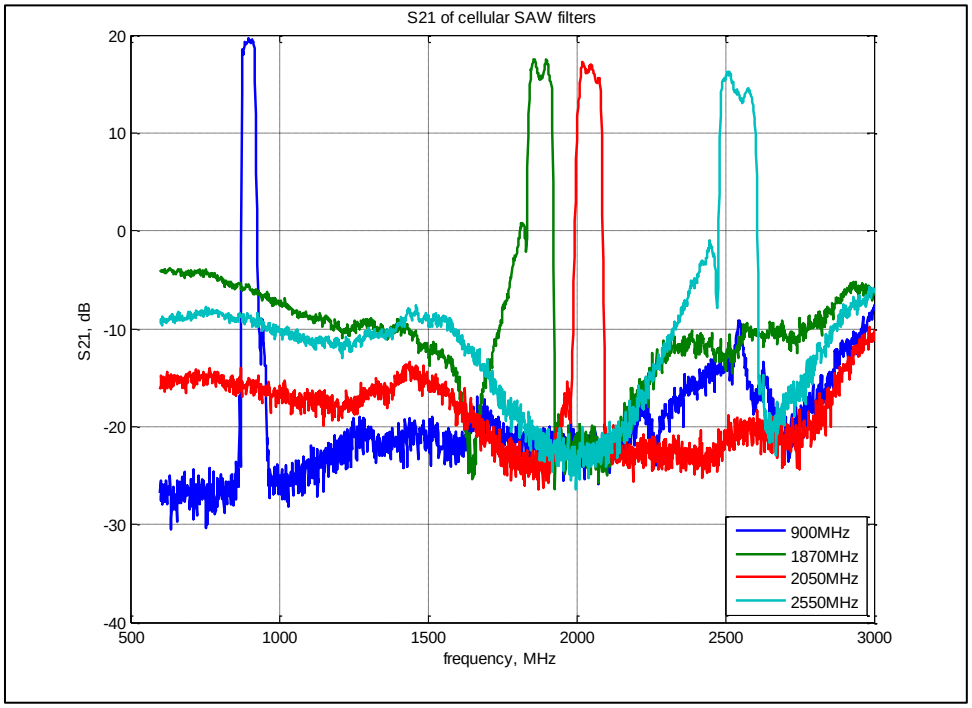

Figure 3.7. SA measurement results for 1880 MHz and 1747 MHz SAW filters.

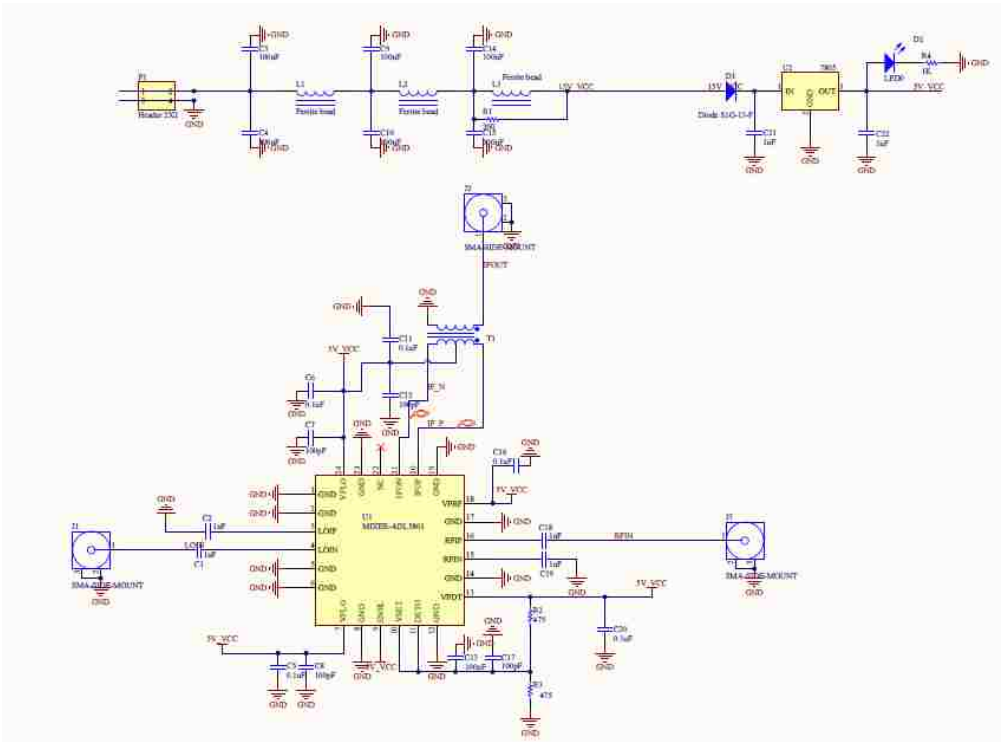

Figure 3.8. Schematic of mixer.

Table 3.2. Measurement results at 900 MHz RF frequency

Frequency	Magnitude
RF=900 MHz	-51.7 dBm
LO=1.3392 GHz	-1.12 dBm
IF=433.92 MHz	-54.4 dBm

Table 3.3. Measurement results at 1900 MHz RF frequency

Frequency	Magnitude
RF=1900 MHz	-52 dBm
LO=2.3392 GHz	-1.67 dBm
IF=433.92 MHz	-54.5 dBm

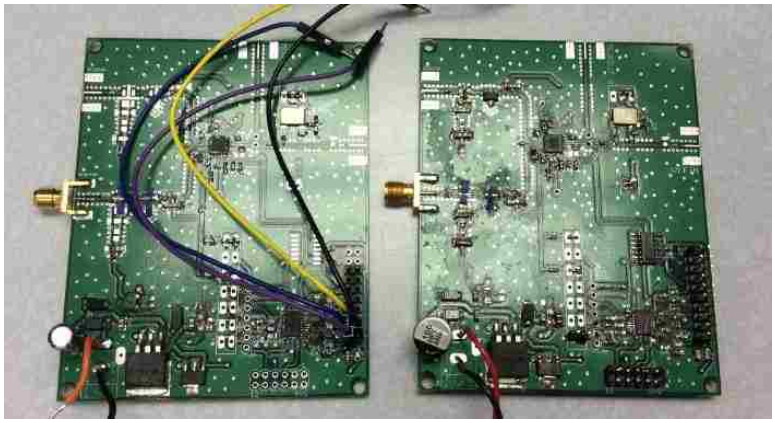

Figure 3.9. Assembled frequency synthesizer board.

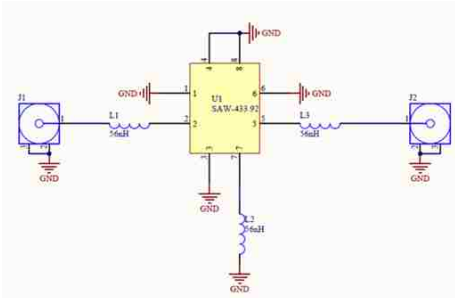

Figure 3.10. Schematic of 433.92 MHz SAW filter and measurement results.

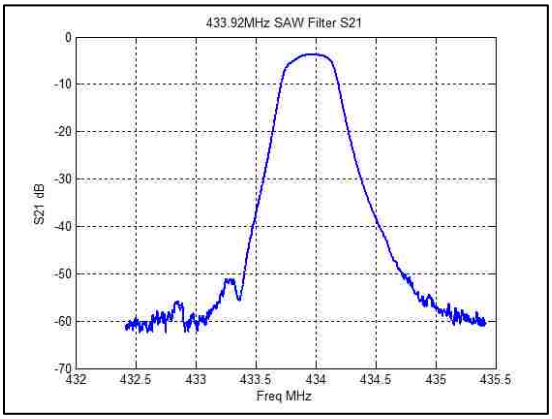

Figure 3.11. Measured S21 of the 433.92 MHz SAW filter

Table 3.4. ECS crystal filter parameters

PART NUMBER *	CENTER FREQUENCY Fo	PASSBAND MIN.		STOPBAND MAX.		ATTENUATION GUARANTEED MIN.		RIPPLE MAX.	LOSS MAX.	TERMINATING IMPEDANCE	OPERATING TEMPERATURE	NO. OF POLES
	MHz	dB	KHz	dB	KHz	dB	KHz	dB	dB	Ω//pF	°C	
ECS-75SMF45A7.5B	45.000	3	± 3.75	30	± 12.5	80	-910	1.0	4.0	350//6.5	-30 ~ +80	4
ECS-75SMF45A20B	45.000	3	± 10.0	25	± 25.0	80	-910	1.0	3.0	500//2.5	-30 ~ +80	4
ECS-75SMF45A30B	45.000	3	± 15.0	30	± 50.0	80	-910	1.0	3.0	1000//1.0	-30 ~ +80	4
ECS-75SMF70.05A20B	70.050 *	3	± 10.0	20	± 25.0	70	-910	1.0	4.0	2500//-1.0	-30 ~ +80	4

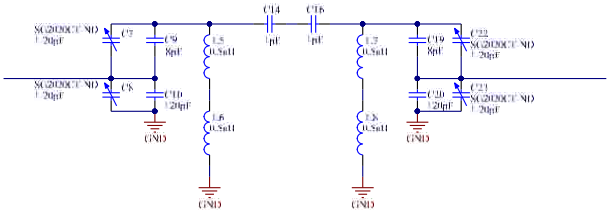

Figure 3.12. Bandpass filter with parameters optimized in ADS.

3.1.7. Second Stage Adjustable Amplifier. In this stage, we used 3 ADL5611 amplifers to generate enough gain (Figure 3.15 and Figure 3.16). We selected ADL5611 because it has rather flat gain of 22dB from 30MHz to 4GHz.

Since the log detector and linear detector have different work range, we need to be able to control the power that goes into the detector. Thus we added a voltage controlled attenuator IC between second and third ADL5611 IC. The attenuator is ALM-38140 from Avago. It has an Input IP3 of 50dBm. It can give about 60dB attenuation at 45MHz.

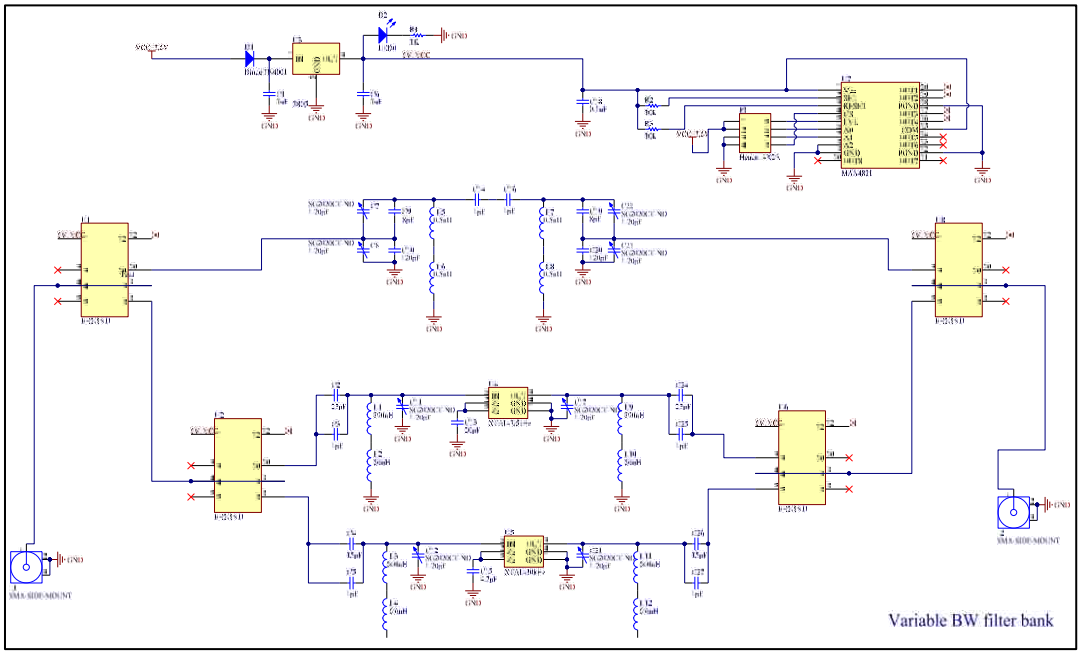

Figure 3.13. Circuit diagram of variable BW filter bank.

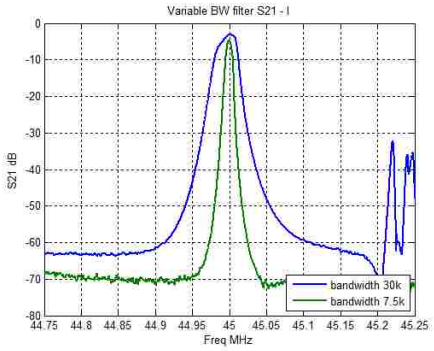

(a)

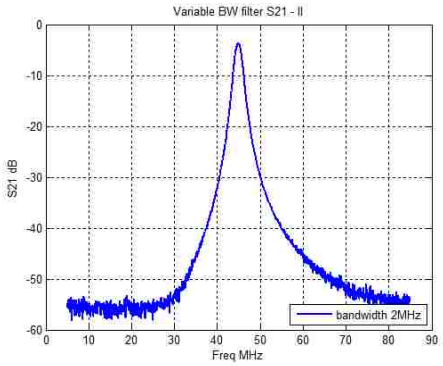

(b)

Figure 3.14. S21 of different filters.
(a) 30 kHz and 7.5 kHz BW filter S21; (b) 1 MHz BW filter S21

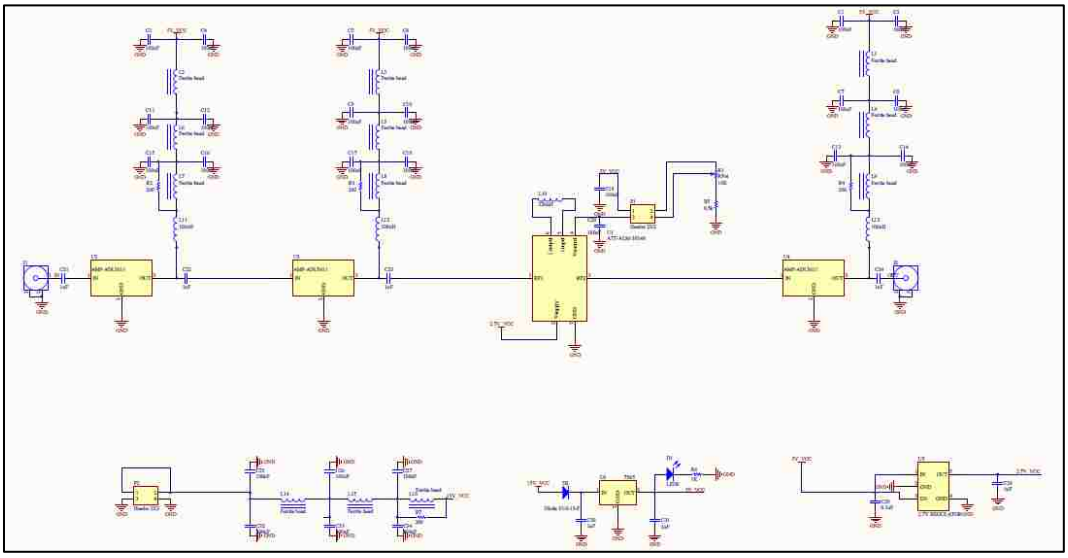

Figure 3.15. Schematic of second stage adjustable amplifiers.

Figure 3.16. Manufacture board of second stage adjustable amplifiers with box.

3.1.8. Amplifier ZKL-1R5+. A ZKL-1R5+ (Figure 3.17) from Mini-Circuits has 40 dB stable gain over 10 to 1500 MHz.

Figure 3.17. Mini-Circuits ZKL-1R5+ 10 to 1500 MHz 40 dB gain amplifier

3.1.9. Splitters. Two splitters (Figure 3.18 and Figure 3.19) from Mini-Circuits were added into the system for the purpose of debugging and measuring signal levels. ZFSCJ-2-4+ 2-way splitter's typical operation range is from 50MHz to 1000MHz, which is used after first mixer (433.92MHz) in the system. ZA3CS-400-3W+ 3-way splitter is from 2MHz to 400MHz, which is used after variable BW filterbank (45MHz).

Figure 3.18. ZFSCJ-2-4+ 2-way splitter.

Figure 3.19. ZA3CS-400-3W+ 3-way splitter.

3.1.10. Detectors. Both a log detector and a linear detector were mounted on the same board. The log detector (Figure 3.20) is an AD8318 which had been well tested in previous measurements. The linear detector (Figure 3.21) is a Schottky Diode HSMS which had also been investigated before.

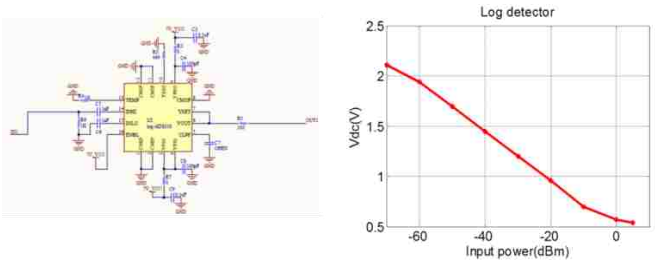

Figure 3.20. Schematic of log detector and measurement result.

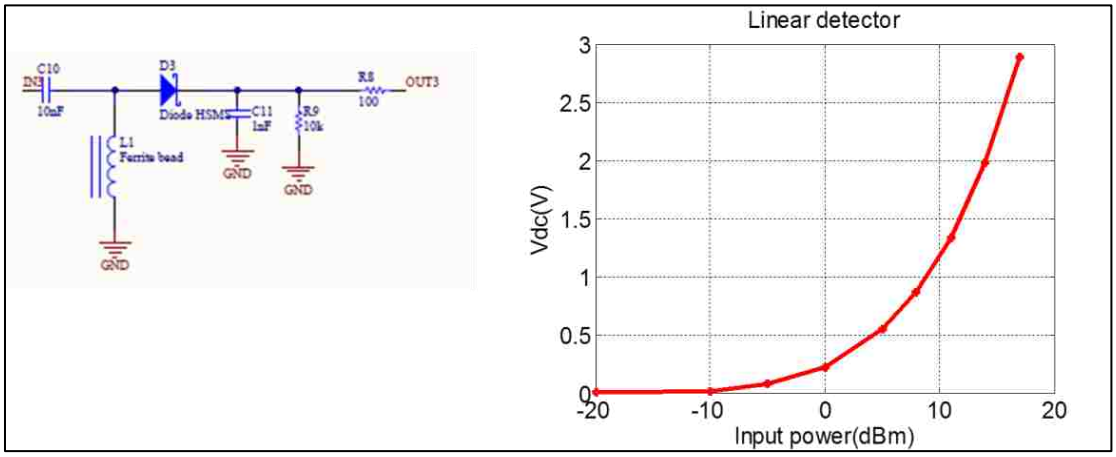

Figure 3.21. Schematic of linear detector and measurement result.

3.1.11. Touchscreen Control Panel. The SmartGLCD touchscreen (Figure 3.22) from MikroElektronika was selected as the control panel for the system. This unit is based on the microcontroller unit (MCU) PIC18F87K22 from Microchip.

Figure 3.22. SmartGLCD touchscreen panel.

The control panel was designed to control the selection of filters on two filter banks, and also output frequency of two MAX2870 frequency synthesizer boards. It also

takes in the power reading from the AD8306 log detector and shows the input power of the detector board.

The user interface on the touchscreen is shown in Figure 3.23 and Figure 3.24. On the first screen (Figure 3.23), the user can set the Tx frequencies. Then, the user has to set the bandwidth of the variable bandwidth filter bank. Typically, for ultrasonic application, the bandwidth should be set to120 kHz.

After setting up Tx frequencies and filter bandwidth, the user can press the ENTER button to send commands to the modules in the system.

The touchscreen will calculate the IM3 frequency and select cellular SAW filters accordingly. It will also calculate input power at the detector board (Figure 3.24).

3.1.12. System Integration.. All modules in the PIM receiver system were integrated into a 17 in x 17 in x 6 x aluminum chassis (Figure 3.25). Because of limited space, some modules were mounted on the side walls. The open frame switching power supplies are covered by a plastic box for protection.

The touchscreen panel was mounted on the side wall. All modules were fixed to the chassis and tested for reliability.

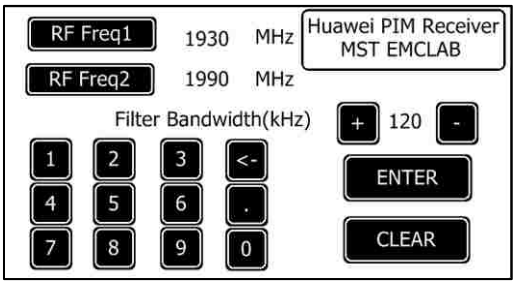

Figure 3.23. First screen of user interface.

Figure 3.24. Second screen of user interface

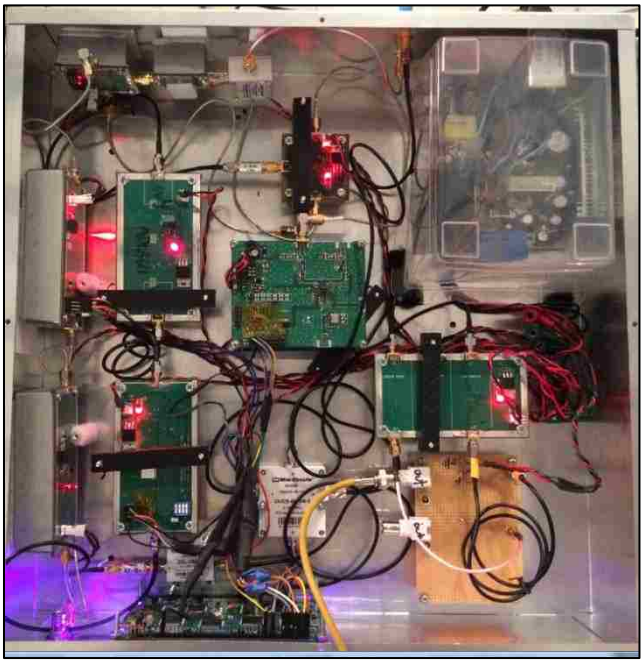

Figure 3.25. Integrated PIM receiver in an aluminum chassis.

3.2. PIM ANALYZER

3.2.1. Self-made PIM Analyzer. During this project, the demo unit Kaelus iQA1800 was sent back to Kaelus, thus, other solutions for PIM analyzer were considered. At the beginning, a PIM analyzer was planned to be built by the EMCLab.

As shown in Figure 3.26, the proposed PIM analyzer consists of two signal generators, two high power RF amplifiers, one power combiner, and one duplexer.

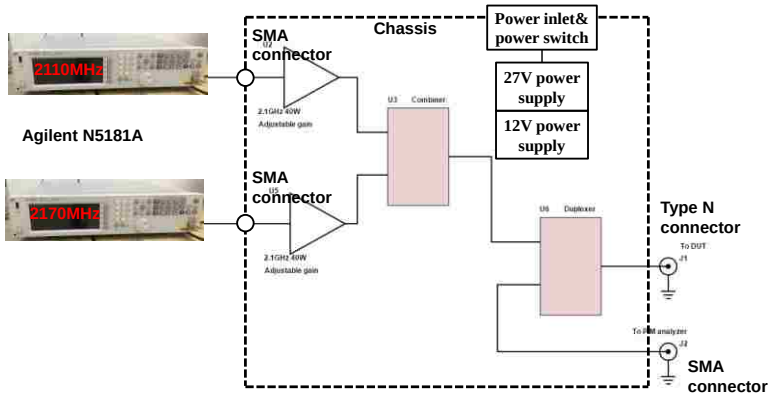

Figure 3.26. Block diagram of self-made PIM analyzer.

Two RF power amplifiers (Figure 3.27) were bought for the PIM analyzer. The amplifiers work at 2100 MHz and have a 46 dBm maximum output power.

The selected power combiner has a working frequency from 300 MHz to 2700 MHz. For the duplexer, the Tx frequencies are 2110 MHz to 2170 MHz, and the Rx frequencies are 2050 MHz to 2060 MHz. However, the PIM level caused by the duplexer was measured to be about -100 dBm (2×43 dBm input) which exceeded the acceptable PIM level for our application.

The low PIM duplexers were not available on the market and would have had to be customized; however, both the time and cost were not acceptable to build a customized low PIM duplexer.

Figure 3.27. Two power amplifier purchased for the self-made PIM analyzer.

3.2.2. Modified PIMPro 1921. Because of the limited time and budget, a commercial used PIM analyzer became the choice. After comparing several models on the market, a used CCI PIMPro 1921 PIM analyzer (Figure 3.28) was acquired**.**

This analyzer works on bands PCS 1900 and AWS 2100. Receive frequencies are 1850-1910 MHz/1710-1755 MHz, transmit frequencies are 1930-1990 MHz/2110-2155 MHz. The adjustable output power range is 17 to 46 dBm × 2.

The major problem for this PIM analyzer was that it didn't have an RF output port and had to be modified before it was able to be used as the vibration modulation method.

The case was carefully opened and the structure was carefully studied (Figure 3.29). It was found that the duplexer did not have the Rx output port with connectors; instead, it only had a pin connecting to the Rx module (Figure 3.30) of the PIM analyzer. A coax probe was soldered to the pin and the ground nearby (Figure 3.31).

The PIM level was able to be measured by using external devices like the spectrum analyzer and self-made PIM receiver.

Another problem was discovered: because of the special characteristics of the vibration modulation method, it is required that the Tx signal phase noise be as low as possible so that the modulated signal could be detected, however, when using the internal signal source the measured phase noise was only about -80 dBc/Hz at 29 kHz away. Such a high phase noise level largely reduced the sensitivity of the method.

Figure 3.28. CCI PIMPro 1921 PIM analyzer.

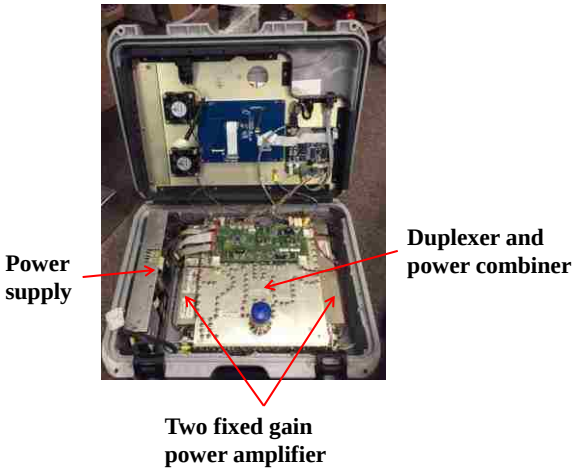

Figure 3.29. Internal structure of the purchased PIM analyzer.

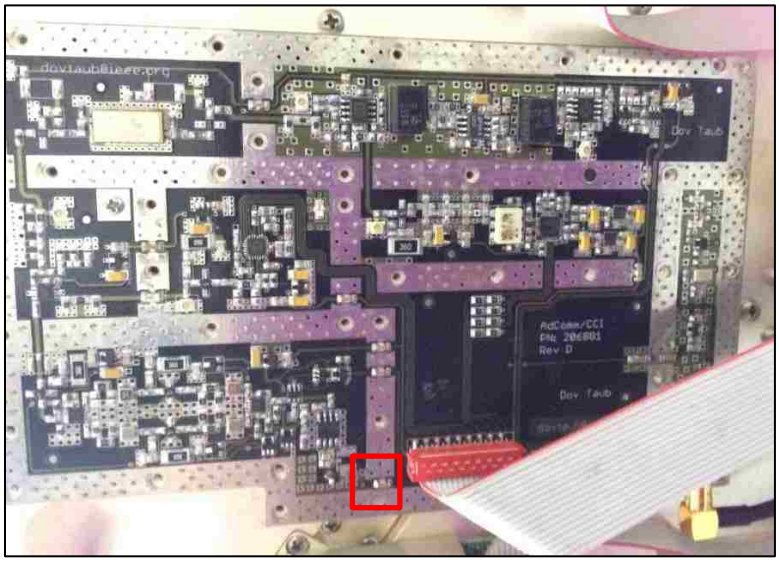

Figure 3.30. Rx module of the PIM analyzer.

Figure 3.31. Modified analyzer with coax probe added for Rx (PIM) signal output.

As shown in Figure 3.32, if the phase noise was the red curve then the modulated signal could not be measured. If the phase noise was the blue curve, the modulated signal could be detected. Thus, it was of our interest to reduce the phase noise as much as possible so two external signal generators were introduced to replace the internal high phase noise signal source. The measured phase noise at 29 kHz away was about -105dBc/Hz.

The modified PIMPro 1921 PIM analyzer system block diagram is shown in Figure 3.33. The two signal sources are Agilent N5181A RF signal generators. The Rx signal was measured at the spectrum analyzer through a coax probe. The complete PIM analyzer set-up is shown in Figure 3.34 and Figure 3.35.

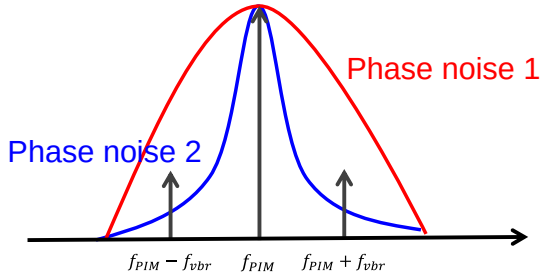

Figure 3.32. Illustration of the effect of different phase noise level.

3.3. PIM VIBRATION SYSTEM

The PIM vibration method system consisted of three modules: an ultrasonic transducer, ultrasonic driver, and signal source.

In the previous tests, it was found that using acoustic speakers as a vibration source would result in very loud noise. Thus, it would be very inconvenient for the user to perform the measurement in such a noisy environment. The speaker's power may also not be high enough. The ultrasonic transducer used in this method was shown in the previous section. Its resonant frequency was about 28 kHz and the maximum output power was about 50W.

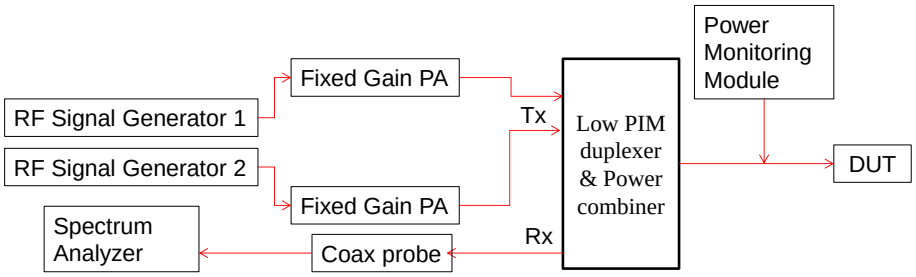

Figure 3.33. Block diagram of the modified PIM analyzer.

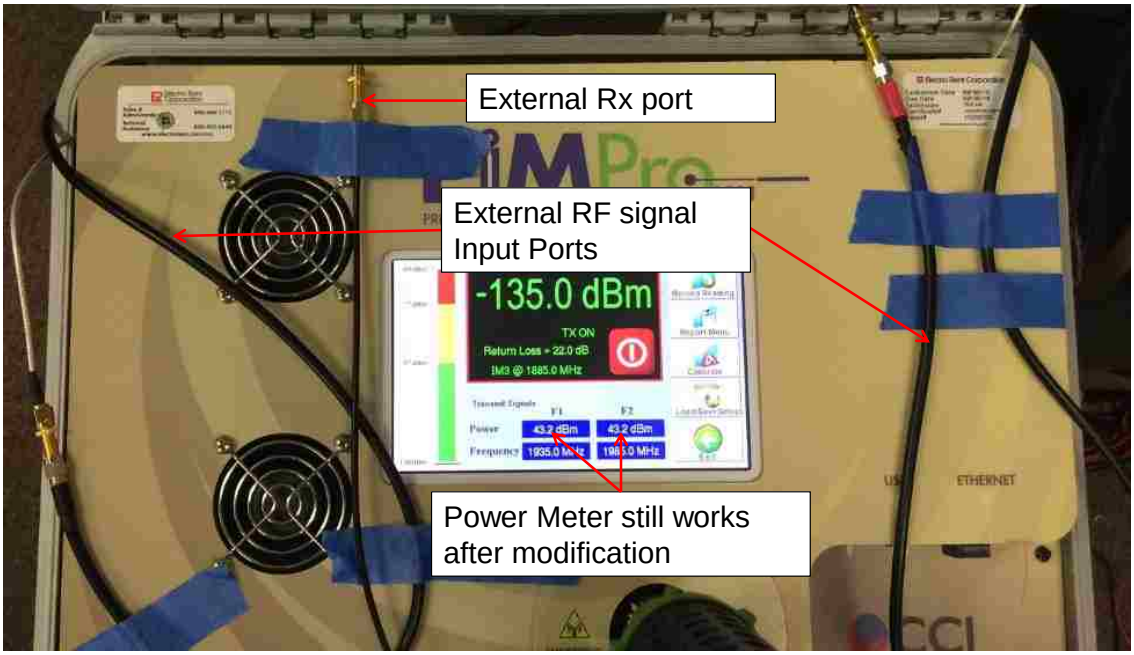

Figure 3.34. Completed modification of PIM analyzer.

Figure 3.35. Photo of completed PIM analyzer modification.

3.3.1. Ultrasonic Driver. At the beginning, an Apex MP118 (Figure 3.36) was selected as the driver amplifier for the ultrasonic transducer. It is a power operational amplifier that can handle 200 V DC supply and is capable of 10 A of continuous output current.

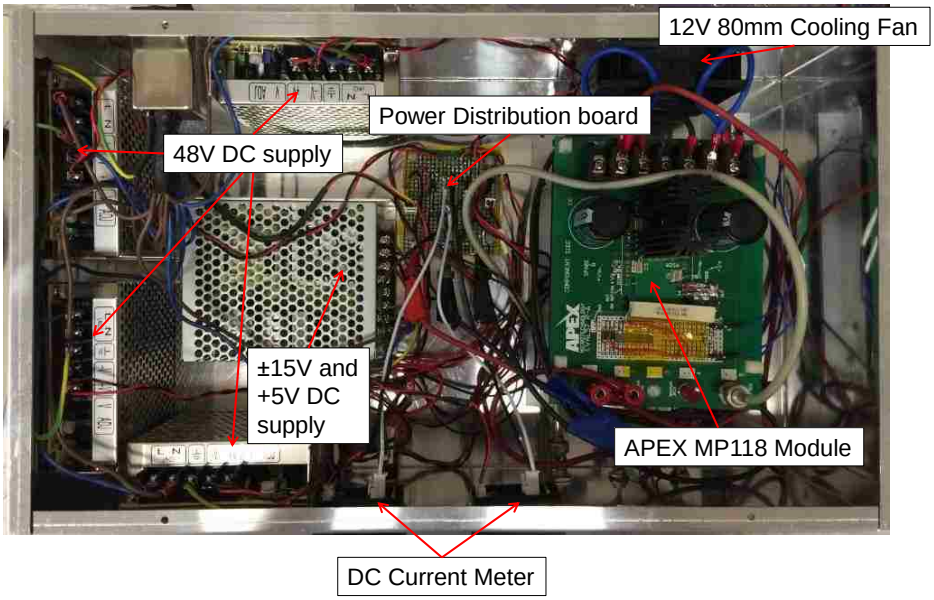

Figure 3.36. MP118 power opamp with power supplies integrated in an aluminum chassis.

During the test, however, the MP118 was damaged twice and was considered to be unstable. Other solutions was taken instead.

3.3.2. Vellaman 200 W Power Amplifier. This power amplifier module can directly use AC power via a transformer (Figure 3.37). Its frequency response is from 3 Hz to 200 kHz (3 dB). This unit has been proven to be robust and easy to use. In addition, a self-made Rogowski coil was made to monitor the output current.

3.3.3. Ultrasonic Transducer. The ultrasonic transducer was introduced in the previous section. A glass tip was attached to the front of the transducer for better vibration delivery to the DUT. A 1:3 transformer was added at the output of the vibration driver for impedance match and to increase the peak voltage on the transducer. The PIM vibration system is shown in Figure 3.38.

Figure 3.37. Assembled vibrator driver with VM100 power amplifier module.

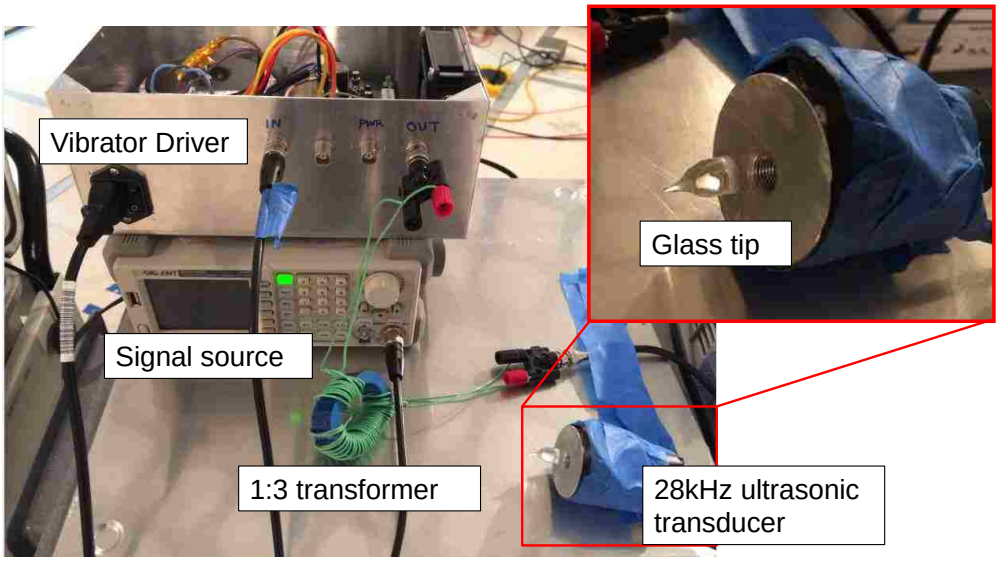

Figure 3.38. PIM vibrator system.

4. PIM VIBRATION SYSTEM TEST AND METHOD VALIDATION

After building the PIM receiver and PIM vibrator system, experiments with a real base station antenna were conducted. The measurements were performed in the 3 m semi-anechoic chamber. The measurement set-up diagram is shown in Figure 4.1 and a photo of the set-up is shown in Figure 4.2.

For the measurement, the PIM analyzer Tx port was connected to the base station antenna via a low-PIM cable. The PIM analyzer, low-PIM cable, and antenna have 7/16 type low-PIM connectors. The two Tx signal were all set to 43 dBm. The modified RF port of the PIM analyzer was first connected to spectrum analyzer (SA). The PIM level was measured at the SA first in order to determine the system PIM level without the intended PIM source. The PIM level could vary from -120 dBm to -90 dBm because of the connection, cable position, and other factors. The PIM level was controlled so that is was steadily under -110 dBm before performing the vibration experiments.

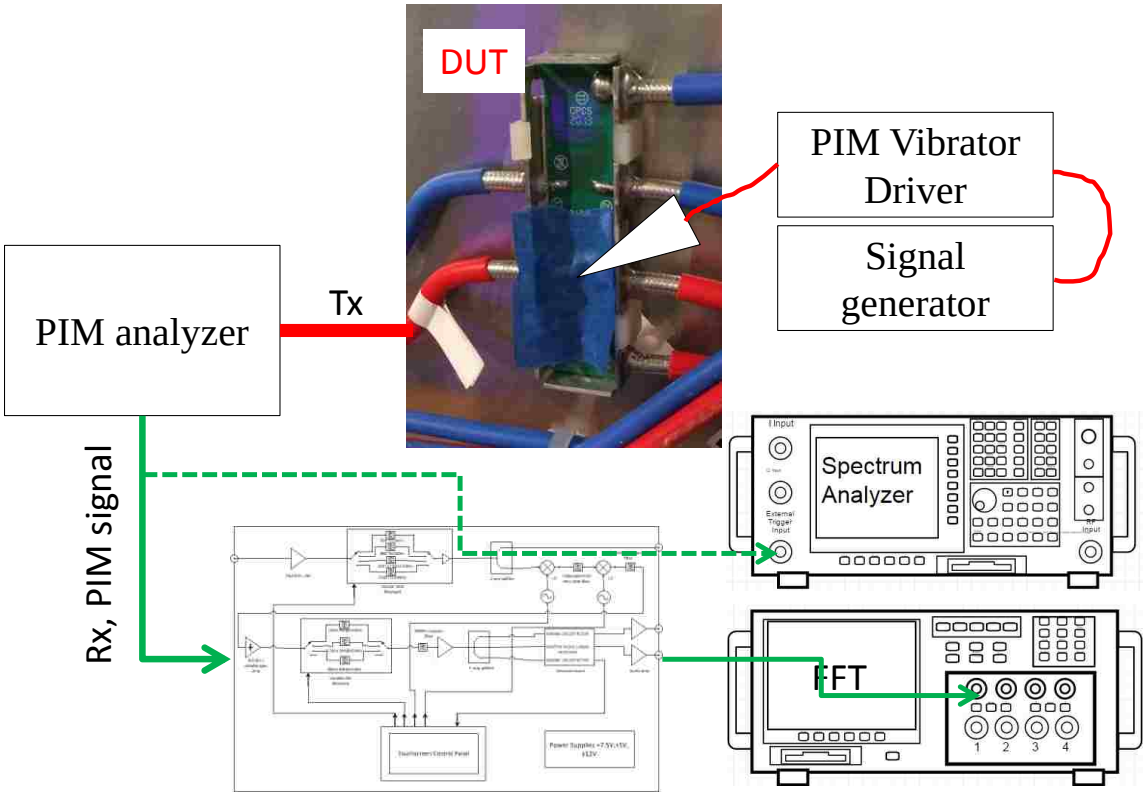

Figure 4.1. Block diagram of measurement set-up.

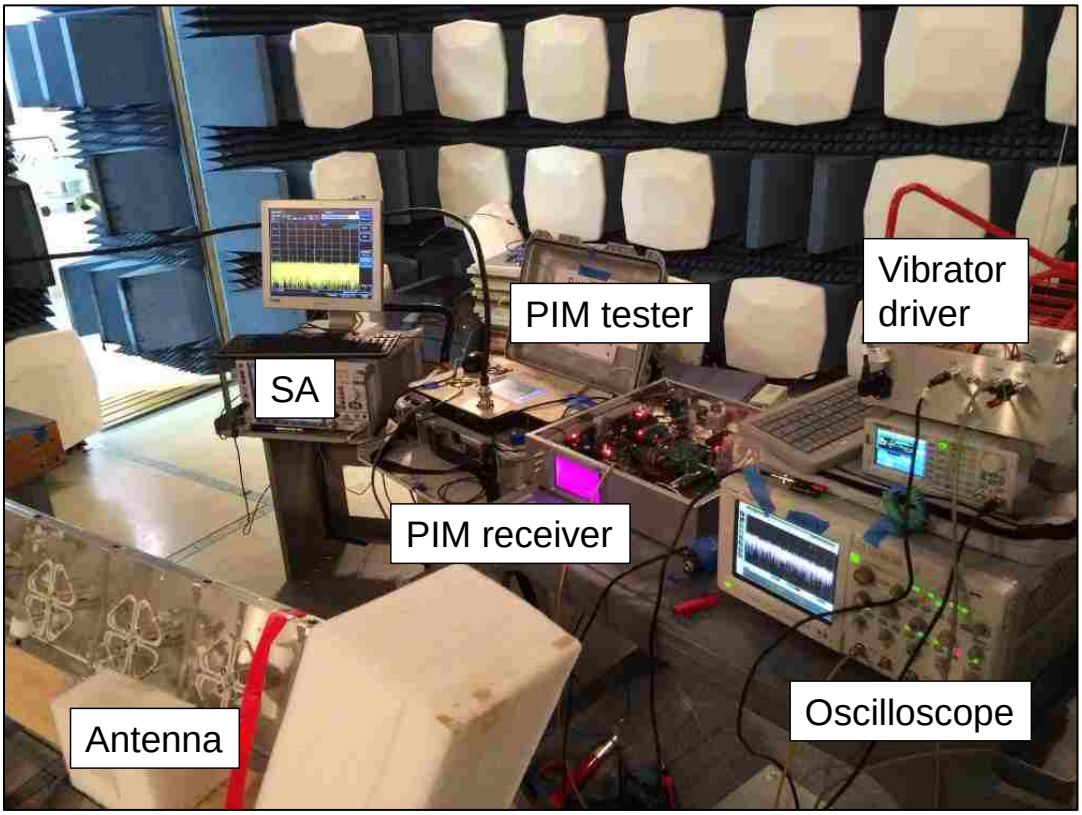

Figure 4.2. Set-up photo of vibration modulation method with base station antenna.

4.1. PIM SOURCE IDENTIFICATION - FERRITE DEBRIS

Different PIM sources were investigated. First, ferrite debris was attached to the splitter section of the antenna on the back. At the splitter, there was a strong EM field due to its structure, thus, a PIM source was created when ferrite material was close to it.

The PIM level before adding the ferrite was <-110 dBm and the PIM level after adding the ferrite was about -100 dBm. The vibration was then applied to different locations, and the modulated signal was only found on the oscilloscope at the PIM source location.

While the vibration method showed very good accuracy in the ferrite experiment (Figure 4.3 and Figure 4.4) since the modulated signal could only be detected at precisely the PIM source location, in reality, the most likely PIM source could be loose contact between metal parts (for example, loose screws or loose connectors). The next experiment tested the loose screws as the PIM source.

Figure 4.3. Ferrite debris as PIM source on power divider.

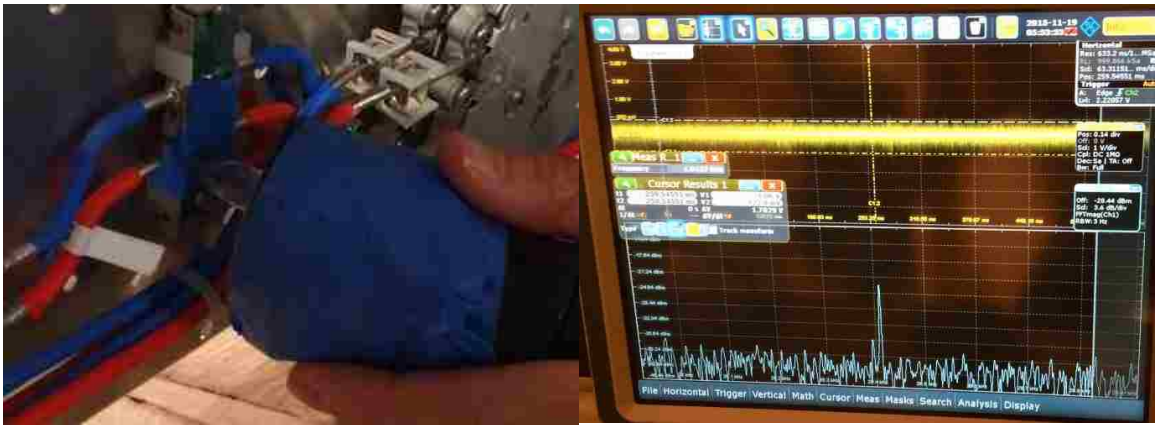

(a)

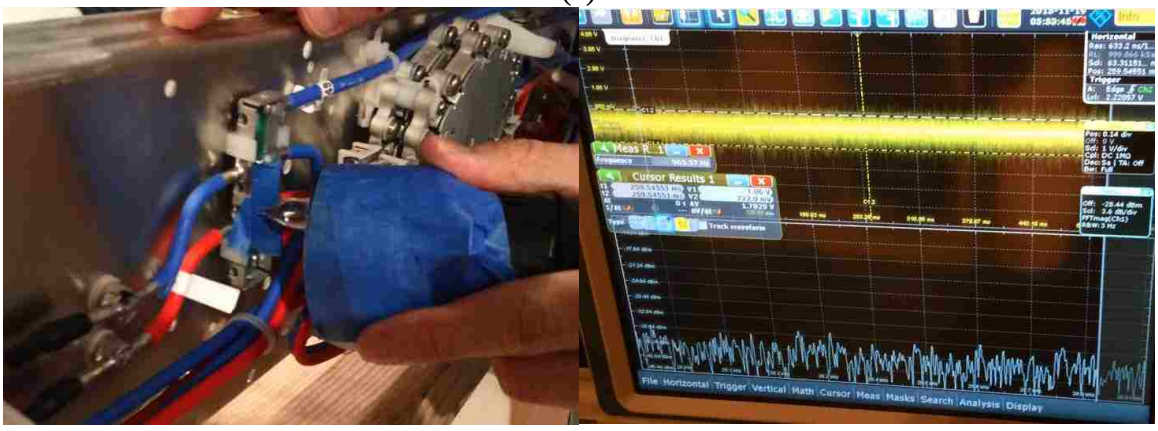

(b)

Figure 4.4. Vibration on different locations: a) vibrated at PIM source point, modulation signal detected; b) vibrated at nearby area, modulated signal not detected

4.2. PIM SOURCE IDENTIFICATION - LOOSE SCREWS

The phase shifter (Figure 4.5) is located in the middle of the backside of the antenna. It is reported that loose screws on the phase shifter or near coax cable are very likely to cause PIM problems. Thus, in this measurement, one screw near the coax cable was intentionally loosened to induce a PIM problem (Figure 4.6).

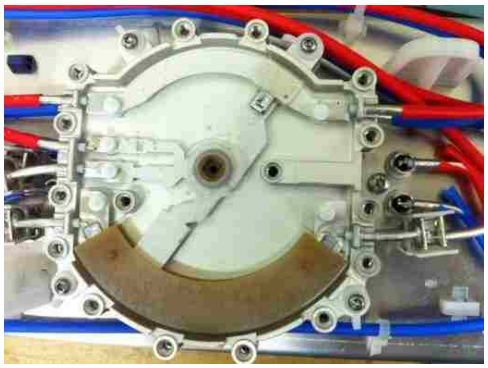

Figure 4.5. Inner structure of E-downtilt (phase shifter).

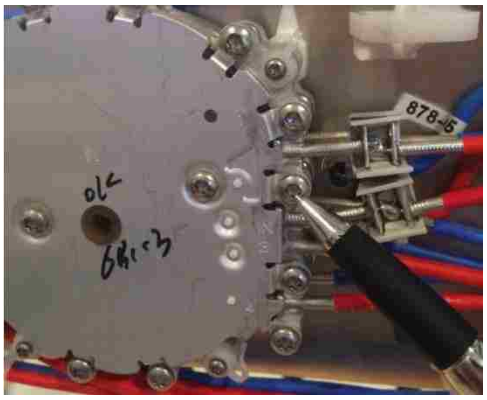

Figure 4.6. Loose screw on the phase shifter as PIM source (indicated by the tip of a pen).

The problem here is that very slight movement of the screw would possibly cause dramatic change in the PIM level. In our test, the PIM level caused by the loose screw would change between -104 dBm to -64 dBm. Thus, it was difficult for us to make a stable PIM source by loosening the screw. These tests were made while the PIM level was about -100 dBm. When vibrating at the PIM source screw, the modulated vibration

signal (28.41 kHz) could be easily observed; while at the neighboring screw, it was harder to detect the signal (Figure 4.7).

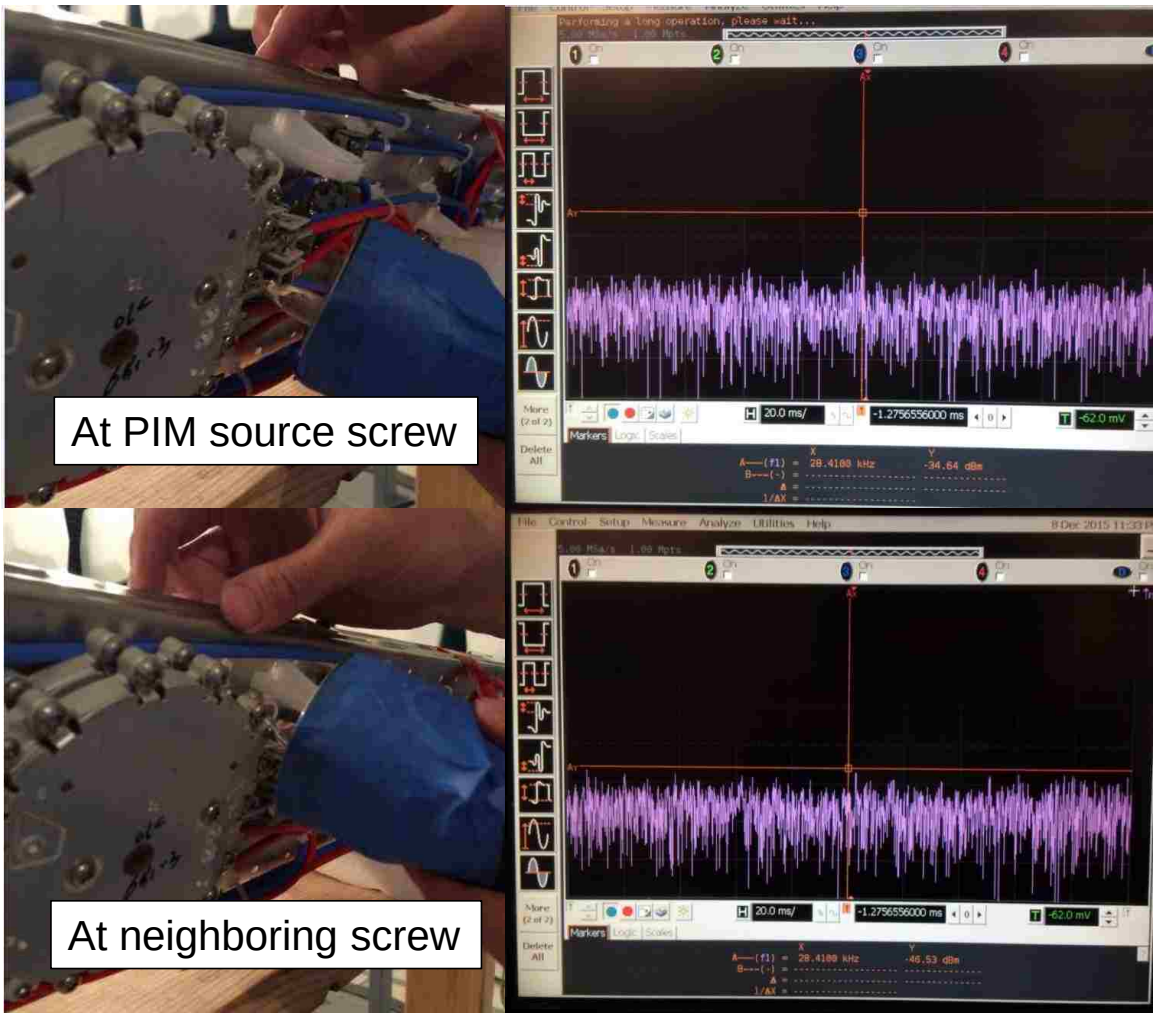

Figure 4.7. Vibrating at different locations on phase shifter.

4.3. CONCLUSION

The vibration modulation method was proposed in this article. The PIM source identification system consists of two subsystems, a PIM receiver and a PIM vibrator. The PIM receiver system was used to increase the SNR of the modulated PIM signal from a PIM analyzer. The PIM vibrator system provides a vibration source for the system. The prototype of the vibration modulation system was built and tested, and then it was tested

in a real case scenario. In this section, the vibration modulation method was tested on the base station antenna. The results show that the proposed method was able to locate the PIM source accurately.

4.4. FUTURE WORK

A second PIM source identification system will be built to accommodate improvements to the first system. Different ultrasonic frequencies will be tested to determine the best frequency for the system. Also, the vibration strength for different types of transducers will be characterized and well documented and new vibration delivery structures will be investigated to replace the glass tip. One of these structures is shown below in Figure 4.8 which consists of a ceramic rod and brass fittings.

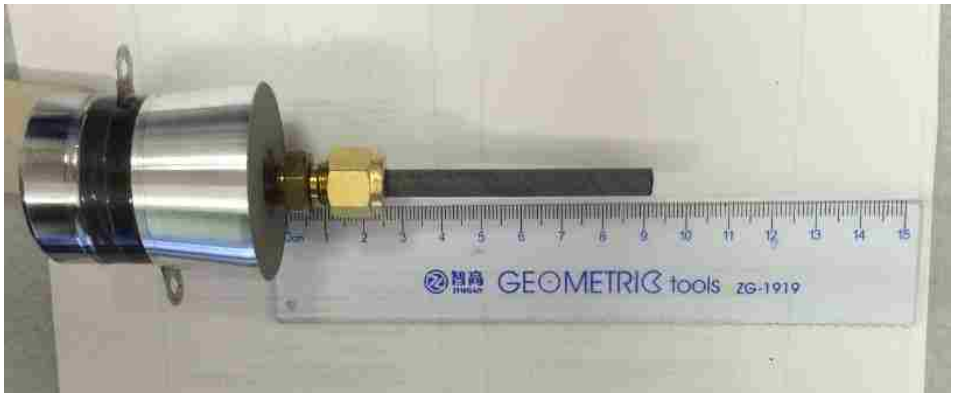

Figure 4.8. Ultrasonic transducer with ceramic rod structure

BIBLIOGRAPHY

[1] Anritsu, "Understanding PIM" [Online]. Available: http://www.anritsu.com/en-US/Products-Solutions/Solution/Understanding-PIM.aspx

[2] Anritsu, "Troubleshooting passive intermodulation problems in the field" [Online]. Available: http://www.electrorent.com/pim-test/pdf/Anritsu-Whitepaper-Troubleshooting-PIM.pdf

[3] Anritsu, "The PIM Source" [Online]. Available: http://anritsu.typepad.com/thepimsource/passive-intermodulation/

[4] D. Weinstein, "Passive Intermodulation Distortion in Connectors, Cable and Cable Assemblies," Amphenol Corporation White Paper, [Online]. Available: www.amphenolconnex.com, http://www.ieee.li/pdf/essay/passive_imd.pdf

[5] IWPC, "Passive intermodulation (PIM) testing best practices", [Online]. Available: http://www.iwpc.org/WhitePaper.aspx?WhitePaperID=18

[6] B. Rosenberger, "The Measurement of Intermodulation Products on Passive Components and Transmission Lines", in Technologies for Wireless Applications, 1999, Digest, 1999, IEEE, MTT-S Symposium, pp57-62

[7] Passive intermodulation, "PIM distortion basics", [Online]. Available: http://www.radio-electronics.com/info/rf-technology-design/passive-intermodulation-pim/basics-tutorial.php

[8] RF Connectors, connector cable assemblies and cables - Intermodulation level measurement IEC 62047

[9] electrorent ,"Troubleshooting passive intermodulation problems in the field", [Online]. Available: http://www.electrorent.com/pim-test/pdf/Anritsu-Whitepaper-Troubleshooting-PIM.pdf

[10] Locating Passive Intermodulation, "PIM Faults", [Online]. Available: http://www.radio-electronics.com/articles/rf-topics/locating-passive-intermodulation-pim-faults-48

[11] Kaelus, "Range to Fault technology", [Online]. Available: http://www.kaelus.com/Kaelus/media/KaelusProducts/Test%20Measurement%20Products/AskOnce/RTF/RTF-white-paper.pdf

[12] Anritsu, "Distance-to-PIM (DTP), Measurement guide", [Online]. Available: http://www.anritsu.com/en-US/Downloads/Manuals/Measurement-Guide/DWL10671.aspx

[13] Anritsu, “Using Distance-to-PIM (DTP) Technology to Speed Site Repairs” [Online]. Available: https://www.youtube.com/watch?v=-DzJEqr3pIA

[14] Mantovani et al. “Apparatus for locating passive intermodulation interference sources,” U.S. Patent 4,648,124, issued Mar. 3, 1987

[15] microwavejournal ,“Passive Intermodulation (PIM) Testing Moves to the Base Station”, [Online]. Available: http://www.microwavejournal.com/articles/11103-passive-intermodulation-pim-testing-moves-to-the-base-station

[16] J. Hesselbarth, “Antennas for cellular base stations,” [Online]. Available: http://www.ihf.uni-stuttgart.de/institut/mitarbeiter/hesselbarth/Vortraege/hesselbarth_artisan_30jan2014_webversion.pdf

[17] MWRF, “Reigning In PIM In Cellular Systems”, [Online]. Available: http://mwrf.com/test-amp-measurement-analyzers/reigning-pim-cellular-systems

[18] Agilent (Keysight) application note, “Innovative Passive Intermodulation (PIM) and S-parameter Measurement Solution with the ENA,” [Online]. Available: http://literature.cdn.keysight.com/litweb/pdf/5991-0332EN.pdf

[19] Keysight, “Passive Intermodulation (PIM) Measurement” [Online]. Available: http://www.keysight.com/main/application.jspx?nid=-33157.0.00&pageMode=OVW&lc=eng&cc=US

[20] CCI, “PIMPro Series” [Online]. Available: http://www.cciproducts.com/www2/index.php/products/pim-analyzers

[21] Boonton, “pim-testers” [Online]. Available: http://boonton.com/products/pim-testers

[22] Rosenberger, “pim” [Online]. Available: http://www.rosenberger.com/en/products/communication/pim.php

[23] Kaelus, “Passive-Intermodulation-PIM-Testing” [Online]. Available: http://www.kaelus.com/Passive-Intermodulation-PIM-Testing/

[24] AWT global, “portable-pim-tester” [Online]. Available: http://www.awt-global.com/pim-test-systems/portable-pim-tester/

[25] Anritsu,” MW82119B”, [Online]. Available: http://www.anritsu.com/en-US/Products-Solutions/Products/MW82119B.aspx

[26] A. P. Shitvov, D. E. Zelenchuk, T. Olsson, A. G. Schuchinsky, and V.F. Fusco, "Transmission/reflection measurement and near-field mapping techniques for passive intermodulation characterisation of printed lines," in Proc. MULCOPIM'08, 2008, paper PIM4, p.1-6

[27] A. P. Shitvov, D. E. Zelenchuk, A. G. Schuchinsky, and V. F. Fusco, "Passive intermodulation generation on printed lines: Near-field probing and observations," IEEE Trans. Microw. Theory Tech., vol. 56, no. 12, pp. 3121–3128, Dec. 2008

[28] S. Hienonen, V. Golikov, P. Vainikainen, and A. V. Räisänen, "Near-field scanner for the detection of passive intermodulation sources in base station antennas," IEEE Trans. Electromagn. Compat., vol. 46, no. 4, pp. 661–667, Nov. 2004

[29] N. Kuga and K. Ohnishi, "Non-contact PIM measurement method for electrical connection inspection," in Proc. APMC'04, 2004, pp. 295-298.

[30] Jameco, "Audio stereo amplifier kit", [Online]. Available: http://www.jameco.com/1/1/924-ebst-11-stereo-amplifier-kit-output-power-1-watt.html

[31] Apexanalog, "Power amplifier for ultrasonic transducer" [Online]. Available: http://www.apexanalog.com/

[32] APC, "apc 90-4040 ultrasonic transducer series" [Online]. Available: https://www.americanpiezo.com/images/stories/content_images/pdf/apc_90-4040.pdf

[33] Digikey, "SAW band pass filter", [Online]. Available: http://www.digikey.com/product-detail/en/CBPFS-1880/744-1443-ND/2685012

VITA

Sen Yang was born in Tangshan, Heibei Prov., China. In 2012, he received B.S. degree in Electrical Engineering from University of Electronic Science and Technology of China, Chengdu, Sichuan Prov., China. He joined EMC Laboratory, Missouri University of Science and Technology in 2013 and worked his M.S. degree. He also worked as a co-op engineer at Cisco EMC design group in 2014. In May 2016, he received his MS degree in Electrical Engineering from Missouri University of Science and Technology. His research interests include IC behavior modeling in ESD event, heatsink radiation model and simulation, passive intermodulation (PIM) source identification.